Microfossils from the lower Mesoproterozoic Kaltasy Formation, East European Platform

Microfossils from the lower Mesoproterozoic Kaltasy Formation, East European Platform

Vladimir N. Sergeev[1], Andrew H. Knoll[2], Natalya G. Vorob'eva[1], and Nina D. Sergeeva[3]

1. Geological Institute, Russian Academy of Sciences, Pyzhevskii per., 7, Moscow, 119017, Russia

2. Department of Organismic and Evolutionary Biology, Harvard University, Cambridge, MA, USA

3. Institute of Geology, Ufimian Scientific Center, Russian Academy of Sciences, Ufa, Russia

* *Corresponding author: Sergeev V.N., Tel. 7-495-959-2923; Fax: 7-495-953-0760; E-mail: sergeev-micro@rambler.ru; Vsergeevfossil@gmail.com*

Abstract

Basinal shales of the lower Mesoproterozoic Kaltasy Formation, sampled from three boreholes drilled into the southeastern East European Platform, Russia, contain abundant and moderately well preserved microfossils. 34 distinct entities have been identified, most assigned to simple sphaeromorphic or small filamentous taxa found widely and characterized by long stratigraphic ranges. Ornamented microfossils found in coastal successions of other lower Mesoproterozoic basins are absent, but large filamentous microfossils interpreted as possible benthic photosynthetic eukaryotes are recorded, drawing comparisons to relatively deep water shales in Siberia. In overall aspect, the Kaltasy microfossils are consistent with other broadly coeval assemblages, but they

highlight the importance of environment, as well as age, in determining the distributions of remains that record the early diversification of marine eukaryotes. *Rectia magna* is described as a new species.

Keywords: Mesoproterozoic, microfossils, biostratigraphy, eukaryotes, East European Platform

1. Introduction

Recent paleontological and biogeochemical research has sharpened our understanding of late Paleoproterozoic and early Mesoproterozoic marine ecosystems. Silicified coastal carbonate facies offer a view of benthic microbes, including abundant and diverse cyanobacteria (e.g., Zhang, 1981; Sergeev et al., 1995, 2007; Kumar and Srivastava, 1995), while carbonaceous compressions in fine-grained siliciclastic lithologies record both benthic and planktonic microorganisms across a range of lagoonal to basinal environments (e.g., Prasad et al., 2005; Nagovitsin, 2009; Agić et al., 2015; Vorob'eva et al., 2015). In many basins of this age, microfossils thought to be eukaryotic are largely restricted to coastal waters (Javaux et al., 2001), and an explanation for this may lie in the physical nature of mid-Proterozoic oceans. Geochemical data on iron-speciation, nitrogen isotopes, and trace metal abundances and isotopes concur in suggesting the surface mixed layer of mid-Proterozoic oceans lay above widespread and persistent anoxic water masses; episodic upward mixing of these subsurface waters may have inhibited eukaryotic diversification in open shelf environments (Anbar and Knoll, 2002; Johnston et al., 2009; Stueeken, 2013; Guildbaud et al., 2015).

Although widespread, subsurface anoxia was not universal in mid-Proterozoic oceans. Basinal shales in the lower Mesoproterozoic Kaltasy Formation, southeastern East European Platform, preserve geochemical evidence that, at least to the depth recorded by maximum flooding, water masses were oxic (Sperling et al., 2014). Here we report on microfossils preserved in Kaltasy shales. The Kaltasy microfossil assemblage preserves both cyanobacteria and eukaryotic microorganisms over a wider range of environments than is typical for microfossils of this age. At the same time, conspicuously ornamented

taxa well known from other, broadly coeval basins are absent, prompting questions about the spatial as well as the time distribution of early eukaryotic microfossils.

PLACE FIGURE 1 NEAR HERE

2. Geological setting

2.1. Tectonic and stratigraphic framework

For many years, Russian geologists have discussed Meso- and early Neoproterozoic stratigraphy in terms of a Riphean stratotype located in the Bashkirian meganticlinorium, a large structure on the western slope of the southern Ural Mountains (Chumakov and Semikhatov, 1981; Keller and Chumakov, 1983; Fig. 1). The term Riphean, currently a formal unit of Russian Stratigraphic Scale, was originally established to encompass a large scale tectonic cycle, comparable to the Phanerozoic Caledonian or Hercynian orogenies (Shatskii, 1964). Later, largely on the basis of stromatolitic assemblages, strata of comparable age were recognized across much of Siberia and the term acquired its present stratigraphic meaning. The Meso-Neoproterozoic succession in the Bashkirian meganticlinorium records the eastern flank of an extensive sedimentary basin that probably graded eastward into a continental margin; it can be correlated with confidence to strata in platform aulacogen (graben, or rift) sections of the adjacent East European Platform. The Uralian part of the basin, representing the margin *per se*, belongs to external part of the Timanian orogeny, deformed in Ediacaran (Vendian) and Late Paleozoic time (Puchkov, 2013).

Regionally, the Mesoproterozoic to lower Neoproterozoic (Tonian and Cryogenian) succession contains up to 15 km of weakly altered sedimentary and subordinate

volcanogenic rocks, divided into the Burzyan, Yurmata, Karatau and Arsha groups, separated by unconformities (the Arsha Group, which occurs only on the eastern limb of the Bashkirian meganticlinorium, was recently added to the Riphean as a result of new isotopic data; Puchkov, 2005, 2013). The entire succession is overlain unconformably by the Ediacaran (Vendian) Asha Group (Fig. 2).

On the western limb of the Bashkirian meganticlinorium, the lower Mesoproterozoic (Lower Riphean) is represented by the Burzyan Group, traditionally divided into the Ai (siliciclastic and volcanogenic rocks, 1500–2000 m thick), Satka (predominantly carbonates 900–1800 m to 2000–2400 m thick, but thinning significantly to the west), and Bakal (shale–carbonate unit, 900–1800 m thick) formations, in ascending stratigraphic order. Their counterparts on the Bashkirian Meganticlinorian eastern limb are the Bolshoi Inzer, Suran and Yusha formations, respectively.

In the Volgo-Ural region to the west, sub-surface Riphean stratigraphy is known from core and geophysical data. The Kyrpy, Serafimovka and Abdulino groups correlate with the Burzyan, Yurmata and Karatau groups, respectively (Fig. 2). The Kaltasy Formation occurs within the Or'ebash Subgroup of the Kyrpy Group (Kozlov et al., 2009, 2011; Kozlov and Sergeeva, 2011). Kaltasy strata include mixed carbonates and shales, correlated with the Satka Formation in the Ural Mountains (Keller and Chumakov, 1983; Kah et al., 2007; Kozlov et al., 2009); the 1230 to 3600 m succession has been subdivided into three conformable members: Sauzovo, Arlan and Ashit. The Sauzovo Member (105 to 816 m thick) consists largely of dolostones that locally contain stromatolites, along with interlayers of dark gray to black shales and less frequent feldspar-quartz siltstones near its base. The overlying Arlan Member (535 to 1216 m thick) is comprised of carbonaceous shales (some of them fossiliferous) and subordinate siltstones, carbonates and dolomitic marls. The Ashit Member (230 to 1550 m thick) consists of dolostones with stromatolite horizons and thin interbedded shales. Fossiliferous samples come from shales of the Arlan

and Ashit members in three cores: 133 Azino-Pal'nikovo, 203 Bedryazh and 1 East Askino (Figs. 1 and 2; Kozlov et al., 2011).

PLACE FIGURE 2 NEAR HERE

As described by Sperling et al. (2014), the Arlan Member in the 203 Bedryazh core (and in 1 East Askino) consists almost entirely of dark, parallel laminated shales with minor, commonly diagenetic micrite/dolomicrite. Clay-rich laminae predominate, with thin intercalations that contain appreciable quartz silt. Fine sand grains of angular quartz occur in some laminae; commonly these float in a finer matrix and may have been transported into the basin by wind. No wave- or current-generated sedimentary structures are present in more than a kilometer of stratigraphic thickness, suggesting persistent deposition below storm wave-base. Consistent with this view, Kah et al. (2007) argued that the 203 Bedryazh drill core penetrates some of deepest Arlan facies found in the entire basin. Kah et al. (2007) also suggested that the cyclic granular dolostones and fine-grained sandstones recovered by the 133 Azino-Pal'nikovo borehole record shallow water, high-energy platform environments near the western limit of the Kama–Belaya aulacogen. Although basinal environments in many lower Mesoproterozoic basins were anoxic, and sometimes euxinic (Sperling et al., 2015, and references therein), Fe-speciation geochemistry of the Kaltasy succession indicates oxic water throughout the range of depths recorded by the succession (Sperling et al., 2014).

2.2. Age of the Kaltasy Formation.

The age of Kaltasy correlatives in the southern Ural Mountains is constrained by the ~1380 Ma Mashak volcanics in the overlying Middle Riphean (Mesoproterozoic) Yurmata

Group (Puchkov et al., 2013; Krasnobaev et al., 2013a) and by ~1750 Ma basalts 200 meters above the base of the Ai Formation (Puchkov et al., 2012, Krasnobaev et al., 2013b). More directly, a series of K–Ar dates obtained for glauconite from the Arlan Member provides ages of 1510, 1520 and 1425 Ma in Borehole 3, Buranovo area; 1488 and 1469 Ma in Borehole 36, Arlan area; and 1358 and 1334 Ma in Borehole 191, Urustamak area (Keller and Chumakov, 1983; all age estimates have an uncertainty of approximately 3%; Gorozhanin, personal communication, 2015). Illite from mudstone of the underlying Norkino Formation penetrated by Borehole 20005 in the Karachevo area, is dated at 1400±42Ma by K–Ar (Gorozhanin, 1995), and K–Ar dates of 1368, 1377 and 1310 Ma were obtained for whole-rock samples of gabbroids that intruded the overlying Nadezhdino Formation (Keller and Chumakov, 1983). Recently Arlan shales were dated using Rhenium-Osmium (Re-Os) geochronology, yielding depositional ages of 1414±40 Ma and 1427±43 Ma for two horizons near the base of the succession (Sperling et al., 2014). In summary, all available geochronological data are consistent with early Mesoproterozoic deposition.

Stromatolites in more proximal facies of the Kaltasy Formation are consistent with geochronological data, recording forms found previously in lower Mesoproterozoic (Lower Riphean) carbonates in the Southern Urals and Siberia (Kozlov et al., 1995). Chemostratigraphic data likewise support an early Mesoproterozoic age (Kah et al., 2007). Microfossils, however, were originally interpreted as supporting a younger age of deposition. Veis et al. (2000) discovered an assemblage of large and relatively complex microfossils in Kaltasy rocks that they termed the Pal'nikov microbiota. As the assemblage differed from known microbiotas of the contemporaneous Satka and Omachta formations, more closely resembling, at least broadly, younger assemblages from Siberia and the southern Ural Mountains, Veis et al. (2000) proposed a Neoproterozoic age of deposition. Since that time, however, both the longer stratigraphic range of many simple

Neoproterozoic microfossils and the importance of facies in Proterozoic micropaleontology have become more fully appreciated (e.g., Sergeev, 1992, 2009; Sergeev et al., 1995, 2010; Kah et al., 2007). Thus, as discussed below, Kaltasy microfossils are fully consistent with an early Mesoproterozoic age.

3. Materials and methods

3.1. Fossiliferous localities.

Microfossils reported in this study occur in shale samples of the Arlan and Ashit members of the Kaltasy Formation collected in 2011 by V.N. Sergeev during joint research with A.H. Knoll, E.A. Sperling, N.D. Sergeeva and the late V.I. Kozlov. The samples were taken from the 203 Bedryazh borehole core extracted near Bedryazh village in the Cis-Ural area (Fig. 1; Google Map Coordinates, decimal degrees latitude and longitude, 56.340809°N, 55.475973°E) and reposited in the BIPiNeft' core storage facility near Kungur; sample depth is shown in Fig. 2. Further Arlan samples come from the 1 East Askino borehole drilled near Askino village in the Cis-Ural area (Fig. 1; 56.093889°N, 56.702778°E) and reposited in the Kuraskovo core storage facility on the outskirts of Ufa; again, sample depths are shown in Fig. 2. Additionally, we examined nine samples of Ashit shale collected by the late A.F. Veis from the 133 Azino-Pal'nikovo borehole (Fig. 1; 56.523374°N, 53.529541°E) obtained from southern Udmurtia, near Izhevsk and partially described by Veis et al.(2000); sample depths are marked in Fig. 2.

3.2. Methods of slide preparation and investigation.

Microfossils were extracted from the shales by low agitation processing. After standard sample processing using approximately 10% concentration (roughly one tablespoon per 100 ml of water) of caustic potash, the shales were dissolved in hydrofluoric acid (100%). Then, acritarchs and other microfossils were collected manually from the residue by a needle using a stereomicroscope. This simple and effective technique avoids the requirement for centrifugation and heavy liquid treatment, facilitating the intact preservation of large microfossils (e.g., Grey, 1999, 2005; Willman and Moczydłowska, 2008; Sergeev et al., 2011). Slide-preparation methods were similar to those described in many previous publications; permanent strew mounts were made using Canada balsam mixed with polypropylene ether to inhibit recrystallization. Microfossils in the maceration slides prepared by A.F. Veis were extracted from rock samples by chemical processing using hydrochloric and hydrofluoric acids in a conventional palynological maceration method, filtering the residue on a 90-µm sieve mesh.

Transmitted-light photomicrographs were acquired using a RME-5 microscope (Rathenower, Germany) equipped with a Canon EOS 300D digital camera (Canon, Tokyo, Japan) and a Zeiss Axio Imager A1 microscope (#3517002390) equipped with an AxioCamMRc 5 digital camera (both Carl Zeiss, Germany).

The microfossils reported in this study were measured using Zeiss Axio Imager A1 microscope Axiovision software. Where appropriate, taxonomic descriptions indicate the mean ("µ") and standard deviation ("σ") for sample populations, the relative standard deviation ("RSD", or standard deviation as a percent of the mean) and number of measured specimens ("n") using SigmaPlot softwear.

3.3. Repository of illustrated specimens.

All specimens discussed and illustrated in this study are reposited in the Paleontological Collection of the Geological Institute of the Russian Academy of Sciences (PCGIN of RAS), Collection # 14712. The sample numbering from the 133 Azino-Pal'nikovo borehole by the late A.F. Veis corresponds to the borehole depth from which samples were taken (Veis et al., 2000).

4. Kaltasy microfossils: taxonomy and biological interpretation

4.1. General characteristics.

The Kaltasy Formation contains abundant organic-walled microfossils of moderate diversity. We recognize 34 distinct entities, largely of sphaeromorph, disphaeromorph and netromorph acritarchs and filamentous forms (Fig. 3). Large and distinctive filamentous and morphologically simple spheroidal fossils dominate the assemblage, including taxa previously described from both lower Mesoproterozoic (e.g., the Lower Member of the Kotuikan Formation, Anabar Uplift, Siberia; Vorob'eva et al., 2015) and upper Mesoproterozoic to lower Neoproterozoic successions (e.g., the Lakhanda Group of the Uchur-Maya Uplift, the Derevnya and Miroedikha formations of the Turukhansk Uplift, and the Inzer Formation of the southern Ural Mountains; Yankauskas, 1989). Most of these taxa have simple morphologies and long stratigraphic ranges, and so they are consistent with radiometric constraints without further constraining depositional age. Ornamented acritarchs found in upper Paleoproterozoic and lower Mesoproterozoic formations elsewhere (e.g., Yin, 1997; Prasad et al., 2005; Nagovitsin, 2009; Adam, 2014; Singh and Sharma, 2014; Agić et al., 2015) have not been identified in the Kaltasy assemblage. Thus, not surprisingly, environment as well as age played a role in determining the composition of Mesoproterozoic microfossil assemblages.

PLACE FIGURE 3 NEAR HERE

4.2. Sphaeromorph, disphaeromorph and netromorph acritarchs.

Unornamented spheroidal microfossils assigned to the form genus *Leiosphaeridia* are abundant constituents of the Kaltasy assemblage. The simple observation that leiosphaerid sizes range from a few microns to more than a millimeter indicates that diversity existed within this component of the assemblage, but formalizing this by recognizing distinct populations and assigning them to discrete species can be challenging because so few characters are available. Yankauskas (1989) addressed this problem by classifying Proterozoic *Leiosphaeridia* according to diameter and wall thickness, inferred on the basis of folding and color pattern. Both color and folding geometry during compression can reflect wall composition as well as thickness, and, of course, color varies as a function of diagenetic temperature. Nonetheless, Yankauskas's framework has found widespread use and we adopt it here as it captures much of the apparent diversity among these populations; we recognize *L. jacutica* (Figs. 4.1, 4.6 , 4.7; diameter 285-800 µm, wall more than 2 µm thick), *L. crassa* (Fig. 4.2, the smaller fossil; diameter 65-70 µm, robust wall with a limited number of large folds), *L. tenuissima* (Fig. 4.2, the larger fossil; diameter 125-135 µm, wall less than 0.5 µm thick), *L. atava* (Fig. 4.5; diameter 360-365 µm, wall 1.5 µm thick), *L. minutissima* (diameter 10-60 µm, wall less than 0.5 µm thick; illustrated in Sperling et al., 2014, Fig. 4.14) and *Leiosphaeridia* sp. (Figs. 4.8-4.10, diameter 135-410 µm, wall about 2 µm thick). We also recognize *L. ternata* (Figs. 4.3, 4.4; diameter 120-190 µm) as a distinctive taxon based on its nearly opaque wall and characteristic radial cracks. Both features are arguably diagenetic in origin, but they appear to reflect a distinctive original wall composition.

Additionally, we consider a population of unusually large sphaeromorphs (diameter 800-1000 µm; Fig. 4.11-4.13; see Section 7). Such large spheroids are commonly lumped together in *Chuaria circularis*, but the Kaltasy fossils differ in key characters from the Grand Canyon populations, including the lectotype designated by Ford and Breed (1973; see discussion in Vidal and Ford, 1985). Specifically, the type population is characterized by an unusually thick wall, with large, thick folds (Butterfield et al., 1994; see also Vidal, 1976), whereas the Kaltasy fossils, while large, had thin walls marked by numerous fine folds. For this reason, we assign the Kaltasy population to *Leiosphaeridia* (?) *wimanii*, reflecting a combination established by Butterfield (in Butterfield et al., 1994) for large, smooth, thin-walled sphaeromorphs. Rare, dark sphaeromorphs with a spongy wall texture are assigned to *Spumosina rubiginosa* (Fig. 5.1, diameter 150-250 µm; Hofmann and Jackson, 1994). The spongy texture is likely to reflect diagenetic alteration.

There is consensus that *Leiosphaeridia* species reflect a variety of biological origins, nonetheless, leiosphaerids have commonly been interpreted as green algae, either the phycomata of prasinophyte green algae (Tappan, 1980) or chlorophyte cell walls (Moczydłowska, 2010; Moczydłowska et al., 2010). Leiosphaerids generally lack ultrastructural features known to be associated with prasinophytes, but a distinctive TLS (trilaminar sheath structure) ultrastructure has been recognized in TEM images of Cambrian and Neoproterozoic specimens, supporting their interpretation as chlorophytes (Talyzina and Moczydłowska, 2000; and, with less certainty, Moczydłowska et al., 2010). This, however, does not mean that all spheroidal acritarchs were sourced by green algae, as potentially preservable spheroidal envelopes are made by organisms ranging from cyanobacteria (e.g., Fairchild, 1985; Sun, 1987; Sergeev, 1992) to ciliates (e.g., Villalobo et al., 2003). Questions of systematic affinity become more challenging in older successions, where the probability of encountering extinct stem group lineages increases substantially. Mesoproterozoic leiosphaerids examined to date do not show recognizably chlorophyte ultrastructures (Javaux

et al., 2004) and so, informed by molecular clocks (e.g., Parfrey et al., 2011; Eme et al., 2014), the range of potential eukaryotic sources for these fossils must include undiagnostic crown group green algae, stem group greens, stem group archaeoplastids (the photosynthetic group that includes green, red, and glaucocystophyte algae), or stem group eukaryotes. In principle, any or all could be represented in the Kaltasy assemblage. C29 steranes, widely accepted as biomarkers for green algae, first become significant constituents of sedimentary organic matter in Ediacaran strata (Knoll et al., 2007; Bhattacharya and Dutta, 2015); thus, if greens are represented among Kaltasy and other early Mesoproterozoic microfossil assemblages, they would appear to have played only a minor role in marine primary production. [Many prasinophytes synthesize mainly C28 sterols, but C28 steranes are also rare or absent in Mesoproterozoic rocks (Kodner et al., 2008).] Aggregates of relatively small (20-35 μm) spheroidal vesicles are identified as *Synsphaeridium* sp. (Figs. 5.2 and 5.3, diameter 20-40 μm). The biological interpretation of this taxon is uncertain and could include cyanobacteria as well as either planktonic or benthic eukaryotes.

PLACE FIGURE 4 NEAR HERE

Three more, broadly sphaeromorphic, disphaeromorphic and netromorphic populations bear mention. First is *Pterospermopsimorpha pileiformis*, a form taxon applied to spheroidal microfossils where one vesicle is encompassed by another. In Figs. 5.4, 5.5 and 5.7, this organization is clearly evident, and it supports the interpretation of these fossils as photosynthetic. In all likelihood, at least one of the preserved walls was vegetative, and living eukaryotes with continuous vegetative walls are nearly all photosynthetic or osmotrophic (Margulis et al., 1990; Teyssèdre, 2006; Moczydłowska et al., 2011). Fig. 5.6 is also tentatively assigned to *P. pileiformis*, but the internal body may represent shrunken cell

contents rather than a distinct wall layer. Found separately, if poorly preserved, the two vesicles of *P. pileiformis* would be assigned to distinct *Leiosphaeridia* species.

We also note the presence of rare elongated vesicles with surfaces that include strips twisted into spiral structures: *Spiromorpha* aff. *S. segmentata* (Figs. 5.8 and 5.9). Similar forms were previously reported from lower Mesoproterozoic shales in China (Yin et al., 2005) and India (Prasad and Asher, 2001), where they were compared to conjugating green algae (Yin et al., 2005). The comparison, however, is broad, and molecular clocks suggest a much later origin of conjugating streptophyte greens (Becker, 2013). Given its rarity and relatively poor preservation, we leave the Kaltasy specimen in open nomenclature.

There are the rare, but distinctive microfossils assigned here to (?)*Moyeria* (Figs. 5.10, 5.11 and possibly 5.12). These large (nearly 200 μm in maximum dimension) vesicles have a strikingly pleated surface of biological origin. The genus *Moyeria* was erected for distinctive Ordovician and Silurian microfossils recovered from fluviatile successions and interpreted as the preserved pellicle of a euglenid protist (Gray and Boucot, 1989). Broadly similar microfossils with longitudinal folds have been figured from nonmarine shales of the 1.1 Ga Oronto Group, Michigan (Wellman and Strother, 2015). Whether these late Mesoproterozoic fossils are euglenids or reflect broad morphologic convergence remains to be established. Given that the Kaltasy fossils are both rare and still further removed from unambiguous *Moyeria* by both time and environment, we remain uncertain of both their formal taxonomic assignment and phylogenetic interpretation. Quite possibly, this fossil represents a new genus and species, but formal evaluation of this awaits the discovery of additional specimens.

Finally, *Navifusa* is a genus name applied to elongate, or netromorph, acritarchs (Hofmann and Jackson, 1994). These fossils are much larger than ellipsoidal fossils called *Archaeoellipsoides*, generally found in silicified carbonates and interpreted as the akinetes of nostocalean cyanobacteria (Horodyski and Donaldson, 1980; Golubic et al., 1995; Sergeev et al., 1995), as well as their at least partial counterpart in shales *Brevitrichoides* (Yankauskas,

1980). The specimen illustrated in Fig. 5.15 closely approximates *N. actinomorpha* from the upper Mesoproterozoic Bylot Supergroup in Baffin Island (Hofmann and Jackson, 1994). The partial specimen in Fig. 5.13 may also fit within this species, but the elongate form in Fig. 5.14 is distinct and can plausibly be interpreted as representing elongation at an early stage of binary cell division. If correct, this would relate the specimen to *Leiosphaeridia* and provide further evidence of a vegetative cell wall.

PLACE FIGURE 5 NEAR HERE

4.3. Large filamentous forms.

Large filamentous forms comprise large, relatively complex microfossils plausibly interpreted as the remains of eukaryotic algae because they exceed the maximal width of known cyanobacterial filaments (~100 µm; Schopf, 1992). Moreover, the constituent cells of the filaments have continuous cell walls, strongly suggesting that the organisms were photosynthetic or osmotrophic. Among living eukaryotes, filaments made of cells with dimensions like those observed in the fossils tend to be photosynthetic, as osmotrophy would be far more efficient with thin filaments such as those of fungial mycelia. They also tend to be benthic. There is no inherent conflict between our interpretation of the environmental setting as basinal and the hypothesis of photosynthesis. Today, benthic multicellular algae grow beneath storm wave base, indeed, at depths greater than 200 m (Littler et al., 1985).

Most important are two groups of large, broadly tubular microfossils with transverse ribs or septa assigned to *Eosolena minuta* (Vorob'eva et al., 2015) and *Rectia magna* sp. nov. Originally described from the upper Mesoproterozoic Lakhanda Formation, the type species of *Eosolena, E. loculosa* (Hermann and Timofeev, 1985)

366 consists of uniseriate filaments, several millimeters long, with constituent cells up to 150
367 µm wide and variably constricted at prominent septum-like transverse walls (Yankauskas,
368 1989; Hermann, 1990; Hermann and Podkovyrov, 2009, 2014; Vorob'eva et al., 2015).
369 *Eosolena minuta*, originally described from the lower Mesoproterozoic Kotuikan
370 Formation, has smaller cells (up to 200 µm wide) but similar organization (Figs. 6.7-6.9;
371 Vorob'eva et al., 2015). For the reasons outlined above, these forms may record benthic
372 photoautotrophs (which does not necessarily make them crown group green algae; see
373 discussion of *Leiosphaeridia*).

374 *Rectia magna* sp. nov., is also large, exhibiting a broadly filamentous organization
375 that widens distally before tapering sharply at its terminus; the wall has thick transverse
376 annulations, ca. 5-7 µm wide (Fig. 6.1-6.6). The size of this population approaches the
377 maximum observed for cyanobacterial filaments, but its overall morphology suggests that
378 *R. magna*, like *E. minuta*, could have been eukaryotic and benthic. A few fossils (Fig.
379 6.10) exhibit broad features comparable to those of *Rectia* but also have a thin surface
380 covering that deforms into tight, thin folds, as observed in the genus *Plicatidium*
381 (Yankauskas, 1989). These may be taphonomic variants of *Rectia magna*; here we
382 differentiate them as *Plicatidium latum* following Veis et al.'s (2000) earlier identification.
383 *Rugosoopsis* sp. (Figs. 6.11 and 6.12) is the name given to non-branching, rigid tubes that
384 bear numerous cross ribs, in contrast to *Plicatidium*, which features elastic tubes bearing
385 cross ribs that are often folded along the primary axis. The affinities of all these fossils
386 remain obscure; however, their large size and relatively complex morphology support an
387 eukaryotic origin.

388

389 **PLACE FIGURE 6 NEAR HERE**

390

391 *4.4. Filamentous microfossils.*

The Kaltasy microfossil assemblage contains abundant and moderately diverse filamentous microfossils less than 100 µm in diameter, most of which can be interpreted in light of the biology and taphonomy of cyanobacteria. Traditionally, uniseriate trichomes with no cell differentiation were placed in the Oscillatoriales (Elenkin, 1949) or Subgroup III (Rippka et al., 1979) of the Cyanobacteria. Molecular phylogenies now make it clear that, as circumscribed, this group is not monophyletic (e.g., Giovannoni et al., 1988; Schirrmeister et al., 2015), but whether simple filamentous multicellularity evolved once within the cyanobacteria and was lost several times (Schirrmeister et al., 2015) or evolved multiple times convergently (Ishida et al., 2001) remains a topic of debate. In either event, the microfossil record of Subgroup III cyanobacteria is one of cellular trichomes, variously well preserved, and extracellular sheaths, and so extant species assigned to *Lyngbya, Oscillatoria*, and related genera provide a morphological basis for interpretation.

Polytrichoides aff. *P. lineatus* Hermann, 1974 (Fig. 7.1), which are bundles of trichomes bound within a common cylindrical sheath, are usually compared with polytrichomous filaments of the oscillatorian genera *Microcoleus*, *Hydrocoleum* or *Schizothrix* (Hermann, 1990; Vorob'eva et al., 2015).

Trichomes composed of disc-like medial cells and rounded terminal cells without encompassing sheaths -- comparable to extant *Oscillatoria* -- are placed in the genus *Oscillatoriopsis*, represented in the Kaltasy assemblage by *O. longa* (Timofeev and Hermann, 1979; Figs. 7.2, 7.6 and 7.7; 22.0-30.0 µm in cross-sectional diameter).

As exemplified by extant Lyngbya, simple trichomes can be encompassed by an extracellular polysaccharide sheath. Sheaths can bear the imprint of trichome cells they once contained, either as distinct collar-like annulations (*Cephalonyx* sp.; Fig. 7.4, 7.8) or as regularly spaced pseudosepta (*Tortunema patomica*, Butterfield et al., 1994; Figs. 7.3, 7.5). Whether each of the form species recognized in the Kaltasy assemblage corresponds

418 to a distinct biological entity is uncertain; differing taphonomic circumstances could easily
419 account for some observed distinctions. Moreover, the boundaries between form genera
420 are porous; all tubular sheaths once contained trichomes and while the distinction between
421 sheaths containing well-preserved trichomes and empty tubes is straightforward, trichomes
422 exhibit a continuum of intermediate preservational states. Nonetheless, classification
423 adopted here captures the morphological variation found within the assemblage.

424 Taphonomic observation and experiments show that cyanobacterial sheaths
425 preserve better than the trichomes they contain (Sergeev and Krylov, 1986; Bartley, 1996),
426 and so tubular sheaths are more common in the Proterozoic fossil record than are
427 trichomes, including in the Kaltasy assemblage. Smooth, non-septate tubes are assigned to
428 the genus *Siphonophycus* (Schopf, 1968; Knoll et al., 1991) and partitioned into species on
429 the basis of size frequency distribution (Butterfield et al., 1994); on this basis, we recognize
430 five species (*S. robustum, S. typicum, S. kestron, S. solidum*, and *S. punctatum*; Fig.3),
431 found as individual fragments or loosely intertwined populations (Figs. 8.4-8.7).

432 Some cyanobacteria form true or false branches, and this can be recorded by
433 branched sheaths; in the Kaltasy assemblage we find scattered fragments of *Pseudodendron*
434 *anteridium* (Butterfield et al., 1994; Figs. 8.1-8.3) that arguably record nostocalean
435 cyanobacteria.

436 In general, then, filamentous microfossils record a diversity of cyanobacteria, many
437 of which lived on the oxic seafloor of the Kaltasy basin, but some of which could have
438 inhabited overlying surface waters.

439

440 **PLACE FIGURE 7 NEAR HERE**

441

442 *4.5. Miscellaneous forms.*

443

PLACE FIGURE 8 NEAR HERE

The Kaltasy assemblage contains additional populations that do not fit into the aforementioned categories. Miscellaneous microfossils include *Pellicularia tenera* (Yankauskas, 1980), relatively large and problematic fusiform vesicles with longitudinal, intertwined thread-like filaments within the body (Figs. 8.8 –8.10), as well as five populations left in open nomenclature. Unnamed Form 1 (Figs. 9.1-9.3) includes translucent, irregular, elongated vesicles with a reticulate surface probably formed during diagenesis. Unnamed Form 2 (Figs. 9.4-9.6) consists of opaque spheroidal vesicles with irregular outlines. Vesicles appear to exhibit blunt conical processes, but we interpret these as products of diagenesis. Unnamed Form 3 (Figs. 9.7 and 9.10) also appears to exhibit small conical spines of uncertain and possibly diagenetic origin. Unnamed Form 4 (Figs. 9.8, 9.9, 9.11 and 9.12) is applied to elongate vesicles often arranged *en echelon*, with two or three connected individuals. Vesicles are translucent to opaque, with a chagrinate surface and, commonly, perpendicular cracks or transverse annulations in the equatorial region. These morphological features are shared by *Pololeptus rugosus*, recently described from Neoproterozoic deposits in China (Tang et al., 2013, see above). Nonetheless, we have chosen to treat these microfossils informally because the transverse annulations could be of diagenetic origin. And finally, Unnamed Form 5 (Figs. 9.13 and 9.14) consists of elongated translucent solitary vesicles composed of two or three segments communicating freely each to other and bearing elongated horn-like protrusions.

PLACE FIGURE 9 NEAR HERE

5. The Kaltasy microbiota in the Mesoproterozoic world

All microfossil assemblages found in upper Paleoproterozoic to lower Mesoproterozoic shales contain simple spheroidal acritarchs and most also contain cyanobacteria-like filaments. Beyond this, however, they can be divided into three broad groupings, based on fossil types not shared among all contemporaneous formations (Vorob'eva et al., 2015). Type I assemblages lack conspicuously ornamented acritarchs but contain abundant small coccoidal (e.g. *Ostiana, Myxococcoides, Synsphaeridium*) and filamentous (e.g., *Siphonophycus, Leiotrichoides, Brevitrichoides*) microfossils not exceeding a hundred microns in diameter; prokaryotic microorganisms account for much of this diversity, as recorded in the Satka and Bakal formations of the southern Ural Mountains and the Omachta and Svetly formations of the Uchur-Maya Region, Siberia (Yankauskas, 1982; Veis and Semikhatov, 1989; Veis et al., 1990; Sergeev and Lee Seong-Joo, 2001, 2004; Sergeev, 2006). Type II assemblages are characterized by the presence of eukaryotic remains with processes or other conspicuous ornamentation, for example, *Shuiyousphaeridium*, *Tappania*, *Valeria, Dictyosphaera* and *Satka favosa*. These taxa have a wide geographic distribution, being reported from the Beidajiang and Baicaoping formations of the Ruyang Group, China (Xiao et al., 1997; Pang et al., 2013; Agić et al., 2015); the Roper Group, Australia (Javaux et al., 2001, 2004); the Chitrakut, Rampur and Deonar formations of the Semri Group and the Bahraich Group, India (Prasad and Asher, 2001; Prasad et al., 2005; Singh and Sharma, 2014); the Newland Formation of the Belt Supergroup, USA (Adam, 2014), and the Dalgokta and Dzhelindukon formations of the Kamo Group, Central Angara Basin, Siberia (Nagovitsin, 2009). Type III microbiotas may share some of the simple coccoids and filaments found in Type I biotas, but additionally include large structures such as *Eosolena, Elatera*, and *Rectia magna*, as observed in the Kotuikan and Ust'-Il'ya formations of the Anabar Uplift, Siberia (Veis et al., 2001; Vorob'eva et al., 2015), and the McMinn Formation of the Roper Group, Australia (Peat et al., 1978).

The Kaltasy assemblage clearly belongs to the Type III grouping. Morphologically complex acritarchs are conspicuously absent, while large filaments like *Eosolena* and *Rectia magna* are equally conspicuously present. The assemblages noted in the previous paragraph are constrained by radiometric dating to fall within a single ca. 200 million year time bloc, but we do not know that they are strictly coeval, leaving open the possibility that differences among assemblages reflect evolutionary change. That said, we think it more likely that differences among assemblages mainly reflect environmental distinctions. Where assemblage composition has been tied to sedimentology and sequence stratigraphy (e.g., Javaux et al., 2001; Vorob'eva et al., 2015), assemblages rich in ornamented acritarchs tend to cluster in near-shore facies. The absence of such fossils in the Kaltasy assemblage could thus reflect the open marine setting of these fossils. The large microfossils that characterize Type III assemblages reflect benthos, probably photosynthetic, growing on the seafloor. In many Paleoproterozoic and Mesoproterozoic basins, basinal shales accumulated beneath anoxic and sometimes sulfidic waters, restricting the environmental amplitude of benthic eukaryotes. In the Kaltasy basin, however, basinal environments were oxic (Sperling et al., 2014), allowing eukaryotes to flourish. Perhaps, then, these assemblages reflect a co-occurrence of moderate depth and oxic waters not broadly observed in basins of this age. Consistent with this interpretation, Type III assemblages of the Kotuikan Formation, Siberia, were deposited during maximum flooding in shales that drape large stromatolitic bioherms; according to Vorob'eva et al. (2015), deposition took place between storm and fair weather wave base. Iron speciation chemistry is not available for this basin but the presence of large, apparently eukaryotic benthos in shales deposited during maximum flooding implies oxic waters in relatively basinal environments.

Sedimentological constraints for Type I assemblages are little explored, but it is likely that all three major assemblage types and variations on these themes reflect

522 deposition along a gradient from near-shore, predominantly lagoonal facies to basinal
523 marine environments deposited beneath tens to more than a hundred meters of seawater.
524 Ecological variation along environmental depth gradients is characteristic of modern
525 oceans, and it has been documented previously in both younger and contemporaneous
526 Proterozoic basins (Knoll, 1984; Butterfield and Chandler, 1992; Javaux et al., 2001).
527 Diversity is commonly highest in mid-shelf environments that are neither restricted by
528 coastal environmental variation nor inhibited by anoxic subsurface waters that mix upward
529 in open marine settings (Veis, Petrov, 1994 a,b; Petrov, Veis, 1995). The hypothesis
530 proposed by Veis et al. (2000) that Kaltasy microfossils are distinct because of their
531 Neoproterozoic age is falsified by radiometric age constraints as well as chemostratigraphic
532 data. Our work, however, helps to explain *why* Veis could have been misled (see also
533 Sergeev et al., 1995), including a greater appreciation that many Proterozoic acritarchs
534 have long stratigraphic ranges and the local, environmentally mediated absence in Veis'
535 assemblages of those few morphologically complex taxa that do seem to be restricted to
536 lower Mesoproterozoic rocks. Paradoxically, associations of evolutionarily conserved
537 cyanobacteria may prove biostratigraphically informative in some Mesoproterozoic
538 successions, because they are closely tied to physical environments that themselves are
539 limited in time (Knoll and Sergeev, 1995; Sergeev et al., 1995; Sergeev, 2006, 2009).
540

541 **6. Conclusion**

542

543 The microbiota of the lower Mesoproterozoic Kaltasy Formation, Cis-Ural Area, East
544 European Platform contains a moderately diverse assemblage of (cyano)bacterial and
545 eukaryotic microorganisms. Kaltasy shales are unusual among Mesoproterozoic strata in
546 recording a depositional environment that was both basinal (but within the photic zone) and
547 oxic, and this helps to explain the distinctive features of Kaltasy microfossils. Thus, the

Kaltasy microfossils provide a fresh reminder that Proterozoic microfossils vary as a function of both time and space, and inferences about evolution or biostratigraphy cannot be drawn in the absence of information about the physical and chemical dimensions of depositional setting. That relatively large multicellular remains occur in basinal, oxic environments indicates that aspects of early eukaryotic evolution may have occurred in environments not commonly sampled by paleontologists (a similar argument has been made concerning early evolution in non-marine environments; Wellman and Strother, 2015). In general, sharper paleoenvironmental and radiometric constraints on informative microfossil assemblages will help us to build a better evolutionary and biostratigraphic understanding of life in mid-Proterozoic oceans

7. Systematic paleontology

7.1. Location of specimens within maceration slides

Figure legends identify the slide containing the fossil, borehole and sample number, location of the specimen within the fossiliferous maceration slide (denoted by the number of the point above the specimen on an overlay-map attached to the palynological slide and by England Finder Slide coordinates for the specimen), and the catalog number of the specimen in the GIN paleontological collection. Thus, for the specimen of *Pseudodendron anteridium* shown in Fig. 8.3, (203B)-40-3, p. 1, E57[3], 14712-86 indicates that the illustrated fossil is from 203 Bedryazh borehole (for borehole index abbreviations see caption to Fig. 1) and occurs in maceration slide 40-3, prepared from rock sample 40 obtained from the Kaltasy Formation (Fig. 2); that within this maceration slide, the fossil occurs at location point 1 and within the England Finder Slide E57[3] area; and that the specimen itself is cataloged as GINPC 14712-86. For the samples collected by the late

A.F. Veis from the 133 Azino-Pal'nikovo borehole, sampled intervals are indicated by sample number. Thus, for the specimen of *P. anteridium* shown in Fig. 8.2, (133AP)-2760-2765-1, p. 4, H36[3], 14712-2764, the sampled interval is 2760-2765.

In this study, we provide the descriptions of new and key importance for Proterozoic paleobiology and biostratigraphy as well as for the taxonomy of the Kaltasy taxa. Well-known and broadly distributed/ long-ranging taxa are not described in detail; however, their morphometric characteristics are briefly provided above.

7.2. Sphaeromorph, disphaeromorph and netromorph acritarchs

Genus *Leiosphaeridia* Eisenack, 1958, emend. Downie and Sarjeant, 1963

Type species: *Leiosphaeridia baltica* Eisenack, 1958

Leiosphaeridia (?)*wimanii* Brotzen, 1941, emend. and comb. Butterfield (in Butterfield et al., 1994)

Figures 4.11, 4.12, and 4.13

Das Fossil aus der Visingsögruppe Wiman, 1894, pl. 5, Figs. 1-5.

Chuaria wimani Brotzen, 1941, p. 258-259.

Kildinella magna Timofeev, 1969, p. 14, pl. 6, Figs. 4-5.

Chuaria circularis Walcott, 1899 (partim): Ford and Breed, 1973, pl. 62, Fig. 3.

Shouhsienia shouhsienensis Xing (Hsing) in Zhang et al., 1991 p. 120, pl. 1, Figs. 16-26.

Chuaria wimanii Butterfield *in* Butterfield et al., 1994, p. 42-43, Figs. 13D-13F (see Zhang et al., 1991, for additional synonymy).

Description: Spheroidal vesicles 800-1000 μm in diameter; walls translucent, about 0.5-1.0 μm thick; surface texture smooth or fine-grained, with numerous fine folds oriented subparallel to cell margin.

Material examined: Nine well-preserved specimens.

Occurrence: Widely distributed in Proterozoic rocks.

Remarks: *Chuaria* is a formal taxon incorporating large spherical microfossils with robust opaque walls that are the remains of either unicellular eukaryotic cells or empty envelopes

of prokaryotic colonies (See Vidal and Ford, 1985; Fairchild, 1985; Yankauskas, 1989; Butterfield et al., 1994; Sergeev, 2006; Sergeev et al., 2012 for additional discussion). Based on SEM observations of material from the type locality, Butterfield in Butterfield et al., 1994, suggested that *Chuaria* should be restricted to spheroidal fossils with wall thicker than 2 µm. We follow the Butterfield et al., 1994, classification here; uncertainty about species attribution reflects a broader uncertainty about how many species of exceptionally large *Leiosphaeridia* may exist.

Leiosphaeridia sp.

Figures 4.8 – 4.10

Description: Solitary, spheroidal, single-walled vesicles 140 to 390 µm in diameter with robust, translucent, chagrinate walls 2 µm thick that are commonly ruptured and exhibit what may be biological openings (n = 8, µ= 225 µm, σ = 103, RSD = 45%). Some vesicles contain a spheroidal cyst-like inclusion up to 350-370 µm in diameter, with a translucent wall 0.5-1.0 µm thick (Fig. 4.9). Vesicle surface fine-grained and smooth, with occasional possible striations.

Material examined: Eight well-preserved specimens.

Discussion: Members of the genus *Leiosphaeridia* are among the most commonly occurring sphaeromorph acritarchs known from Precambrian sediments. Like *Valeria,* this population shows both medial splits and, occasionally, a striation-like surface pattern. Recently Pang et al. (2015) suggested that in *Valeria* the striation-like surface functioned as a mechanism to guide biologically programmed excystment through medial split. In our specimens, however, possible striations could be diagenetic, and so we prefer to classify this form as *Leiosphaeridia* sp.

(?) Genus *Moyeria* Thusu, 1973

Type species: *Moyeria cabottii* (Cramer, 1970), emend. Miller and Eames, 1982

(?)*Moyeria* sp.

Figures 5.10, 5.11 and 5.12?

Leiosphaerid with multiple folds: Sperling et al., 2014, Figs. 4.4 and 4.4a

Description: Vesicle ellipsoidal, fusiform or spindle-shaped; wall consisting of 14 well developed pleats twisted spirally and oriented parallel to the vesicle's longitudinal axis. Pleats overlapping without intermediate space, but also without septa or diaphragm. Vesicle 240 µm long and 200 µm wide; pleats 5-18 µm wide. Vesicle translucent, with psilate surface; wall about 1 µm thick.

Material examined: One well-preserved specimen and another problematic vesicle.

Remarks: This form is similar to *Moyeria* species described from the Paleozoic deposits (Molyneux et al., 2008; Le Hèrissè et al., 2013) and interpreted as euglenid pellicles. However, only one well-preserved specimen has been found and therefore we defined it as (?)*Moyeria* sp. Whether it bears any close phylogenetic relationship to Paleozoic populations is unclear.

Genus *Navifusa* Combaz et al., 1967

Type species: *Navifusa bacilla* (Deunff, 1955).

Navifusa sp.

Figures 5.13 – 5.15

Description: Solitary single-layered nonseptate ellipsoidal vesicles with rounded ends. Vesicle walls translucent to opaque, coarse-grained, 1.0-2.0 µm thick. Ellipsoids 300-550 µm long and 190-375 µm wide (n=3); length/width ratio 1.7-1.5.

Material examined: Nine variously preserved specimens.

Remarks: These ellipsoidal microfossils from the Kaltasy Formation were identified in open nomenclature as *Navifusa* sp. They are larger than ellipsoidal akinetes of nostocalean

cyanobacteria *Archaeoellipsoides* (= *Brevitrichoides*), which can be abundant in Mesoproterozoic peritidal facies (Sergeev et al., 1995); most likely, the Kaltasy specimens are the remains of eukaryotic microorganisms. We cannot exclude the possibility that some specimens assigned to *Navifusa* sp. (e.g., Fig. 5.14) are sphaeromorphic vesicles elongated in an early stage of binary cell division.

Genus *Pterospermopsimorpha* Timofeev, 1966, emend. Mikhailova and Yankauskas, in Yankauskas, 1989

Type species: *Pterospermopsimorpha pileiformis* Timofeev, 1966

Pterospermopsimorpha pileiformis Timofeev, 1966, emend. Mikhailova, in Yankauskas, 1989

Figures 5.4 – 5.7

Pterospermopsimorpha pileiformis Timofeev, 1966, p. 34, pl. 5, Fig. 12; Mikhailova *in* Yankauskas, 1989, p. 49–50, pl. 3, Figs. 7 and 8; Veis and Petrov, 1994a, pl. 3, Fig. 15; Sergeev and Lee Seong-Joo, 2004, p. 18, pl. 3, Figs. 1–3, and 9; Sergeev, 2006, p. 231, pl. 30, Figs. 1-3, and 8; Sergeev et al., 2008, pl. 7, Figs. 1 and 2; Sergeev and Schopf, 2010, p. 395, 396, Figs. 15.1, 15.2, 15.4, and 15.5; Vorob'eva et al., 2015, p. 217, 218, Figs. 8.7, 8.9, and 8.10.

Description: Solitary spheroidal vesicles 110 to 315 μm in diameter (n = 7, μ= 130μm, σ = 96, RSD = 74%), defined by single-layered, 0.5- to 1.0-μm-thick, medium-grained walls, which contain a large, opaque, more or less spheroidal body 95-180 μm in diameter (n = 8, μ= 123μm, σ = 38, RSD = 30%), with a chagrinate superficial texture.

Material examined: Fifteen moderately well-preserved specimens.

Occurrence: Widely distributed in Meso- and Neoproterozoic microfossil assemblages.

Remarks: A well-known disphaeromorph acritarch, *Pterospermopsimorpha*, differs from sphaeromorph acritarchs by the presence a dark robust cyst-like inner body approximately 2/3 of the outer vesicle diameter. *Pterospermopsimorpha pileiformis* differs from other species of *Pterospermopsimorpha* by its vesicle size and by the chagrinate surface of the

inner body (Yankauskas, 1989). The specimen illustrated to Fig. 5.7 is similar to *Simia*, with a flap-like membrane surrounding an inner translucent body, but it also could turn out to be poorly preserved *Leiosphaeridia* with a collapsed inner envelope layer.

Pterospermopsimorpha and the morphologically similar, predominantly Paleozoic taxon *Pterospermella* are commonly interpreted as phycomata of prasynophyte algae (Teyssédre, 2006; Moczydłowska et al., 2011). This is reasonable for Paleozoic forms, but morphology in Proterozoic populations assigned to *Pterospermopsimorpha* is generally quite simple and so might have been generated by a number of distinct groups (e.g., amoebas, see Margulis et al., 1983, Figs. 5D, 5H and 20B). Teyssédre (2006) considered that the name *Pterospermopsimorpha* was a waste-basket for many Precambrian acritarchs in which the so called wings are actually degraded protoplasmic residues. Not surprisingly, *Pterospermopsimorpha* has been reported from numerous silicilastic units ranging in age from early Mesoproterozoic through late Neoproterozoic. Disphaeromorphic *Pterospermopsimorpha*-like morphologies are common among Proterozoic silicified chroococcacean cyanobacteria where a central translucent sphere formed as a result of an inner sheath layer during post-mortum alteration (e.g., Knoll and Golubic, 1979, Fig. 6A-E; Sergeev, 2006, pl. 26, Figs. 1-9; pl. 40, Figs. 11, 12 and 15; pl. 41, Figs. 2 and 3; Sergeev et al., 2012, pl. 7, Figs. 1-6; pl. 8, Figs. 9, 10 and 13).

Genus *Spiromorpha* Yin et al., 2005

Type species: *Spiromorpha segmentata* (Prasad and Asher, 2001)

Spiromorpha aff. *S. segmentata* (Prasad and Asher, 2001) emend. and comb. Yin et al., 2005

Figures 5.8 and 5.9

Navifusa segmentatus Prasad and Asher, 2001, p. 77, pl. 5, Figs. 4, 5, 14 and 15.

Spiromorpha segmentata Yin et al., 2005, p. 57, 60, Figs. 5.1, 5.4-5.8.

Description: Vesicle ellipsoidal, straight, empty inside, consisting of 7-12 strips twisted helically from one end to the other. Strips connected closely without any intermediate space and without septa or diaphragm in the vesicle interior, but with prominent connecting welds forming upraised crescent-like structures (Fig. 5.9, marked by arrows). Vesicle length about 125 µm, vesicle width 45-55; spiral strips 7.5–9.5µm wide, welds 0.5-1.5 µm and upraised 1.5-2.5 µm above main vesicle body. Vesicle surface smooth; wall fine grained about 1 µm thick.

Material examined: One indifferently preserved specimen.

Remarks: The Kaltasy form is similar to *S. segmentata*, but differs slightly in the presence of upraised welded zones connecting adjacent strips. *Spiromorpha segmentata* has been reported from the middle part of the Beidajian Formation, upper Mesoproterozoic Ruyang Group, Shanxi Province, China, and the Sarda and Avadh formations of the Ganga Basin, India (Prasad and Asher, 2001). *Spiromorpha* has compared to modern conjugating green algae, but this comparision is superficial, and molecular clock inferences suggest that conjugating algae diverged as much as 700 million years after the time of Kaltasy deposition (Becker, 2013). We previously identified this Kaltasy specimen as *Brevitrichoides bashkiricus*, misled by its poor preservation (Sperling et al., 2014, Figs. 4.6 and 4.6a).

7.3. Large filamentous forms

Genus *Eosolena* Hermann in Hermann and Timofeev, 1985

Type species: *Eosolena loculosa* Hermann (in Hermann and Timofeev, 1985).

Eosolena minuta Vorob'eva and Sergeev in Vorob'eva et al., 2015

Figures 6.7 – 6.9

Eosolena loculosa Hermann in Hermann and Timofeev, 1985 (partim): Veis et al., 2001, Fig. 2 ж.

Large trichome-like fossils: Veis and Petrov, 1994a, pl. 3, Figs. 1-3, 8, 10, 11, and 13; Veis et al., 2001, Fig. 2 т.

Eosolena minuta Vorob'eva and Sergeev in Vorob'eva et al., 2015, p. 215, Figs. 6.3-6.5.

734 *Description*: Compressed, unbranched tubes separated by cross-ribs into partially isolated
735 isometric chambers that communicate freely each with each other. Tubes with 90-160 μm
736 cross-sectional diameters, up to 360 μm long (incomplete specimen); tube walls translucent,
737 variably constricted at prominent transverse walls, medium-grained, ca. 1-2 μm thick. Cross-
738 ribs opaque, 3-5 μm (possibly up to 9 μm, but this isn't clearly visible) wide and 2-10 μm
739 high; distance between cross-ribs ranges from 20 to 30 μm.
740 *Material examined*: Five variously preserved specimens.
741 *Occurrence*: Early Mesoproterozoic: Kotuikan Formation, Anabar Uplift, Siberia; Kaltasy
742 Formation, Cis-Urals area, East European Platform.
743 *Remarks*: *Eosolena minuta* differs from *E. loculosa* and from *E. anisocyta* Hermann (in
744 Hermann and Timofeev, 1985) in the smaller cross-sectional diameter of tubes: 75-205 μm
745 vs. 200-800 and 450-750 μm, respectively, and from *E. anisocyta* in a lack of clear
746 separation of the thallus into chambers (Yankauskas, 1989).
747
748 Genus *Plicatidium* Yankauskas, 1980
749 *Type species*: *Plicatidium latum* Yankauskas, 1980
750 *Plicatidium latum* Yankauskas, 1980
751 Figure 6.10
752 *Plicatidium latum* Yankauskas, 1980, p. 109, 110, pl. 12, Fig. 15; Yankauskas, 1989, p. 139, pl. 41, Figs. 3
753 and 4; Veis et al., 2000, pl. 2, Fig. 10; Sergeev et al., 2007, pl. 1, Fig. 19; Pang et al., 2015, Figs. 2A and 2B;
754 Vorob'eva et al., 2015, p. 216, Figs. 6.6-6.9.
755 *Description*: Compressed, unbranched tubes with thin elastic walls bearing numerous elastic
756 cross-ribs or fine folds broadly perpendicular to the tube axis. Tubes 160-170 μm in cross-
757 sectional diameter, up to 135 μm long (incomplete specimen); tube walls translucent,
758 medium-grained, ca. 1 μm thick. Ribs opaque, 1.0-2.0 to 3-4 μm wide and 0.5-1.5 μm high;
759 distance between ribs ranges from 5.5 to 7.5 μm.

760 *Material examined*: Two well-preserved specimens.

761 *Occurrence*: Widely distributed in Proterozoic microfossil assemblages.

762 *Remarks*: We do not accept the emendation and merging of *Plicatidium* and *Rugosoopsis*
763 suggested by Pyatiletov, 1988 and Butterfield et al., 1994, as both the details of
764 morphology and mechanical properties of the two entities differ (rigid vs. elastic tubes; see
765 Sergeev et al., 2007 and Vorob'eva et al., 2015, their Figs. 4C and 4D). Recently Pang et
766 al., 2015 suggested a secondary origin for *Plicatidium* folds.

767

768 **PLACE FIGURE 10 NEAR HERE**

769

770 Genus *Rectia* Yankauskas, 1989

771 *Type species*: *Rectia costata* (Yankauskas, 1980) comb. Yankauskas, 1989

772 *Remarks*: *Rectia* was erected by Yankauskas in 1989 on the basis of sheaths with
773 annulations earlier described as *Siphonophycus costatus* (Yankauskas, 1980, 1982). The
774 genus suffered many subsequent revisions and was considered as a junior synonym of
775 *Cephalonyx* (Butterfield et al., 1994) or *Rugosoopsis* (as *Siphonophycus costatus,*
776 Moczydlowska, 2008). We consider *Rectia* to be a distinct morphological entity, differing
777 from *Rugosoopsis* by its pseudocellular, filamentous nature (in contrast to rugose surface of
778 *Rugosoopsis* and *Plicatidium)* and by its paired ring-like annulation (in contrast to large
779 isometric cells or cell-casts of *Cephalonyx).* Earlier, similarly large pseudocellular
780 filaments were described as *Striatella coriaceae* Asseeva (in Asseeva and Velikanov,
781 1983), but an earlier homonym (Mädler, 1964) renders this generic name illegitimate (see
782 Butterfield et al., 1994). *Botuobia* Pyatiletov, 1979 is another genus of morphologically
783 similar filamentous microfossils embracing mainly sheaths with trichome cell imprints of
784 large diameter. *Botuobia magna* (Tynni and Donner, 1980) exceeds 100 µm in diameter
785 but is still smaller than *Rectia magna*; moreover, its surface is covered with septate cell

786 casts without doubled annulations. Veis et al. (2000) identified these microfossils as
787 *Botuobia*, a taxon now considered to be a junior synonym of *Tortunema* (Butterfield in
788 Butterfield et al., 1994). Therefore, we have chosen describe the Kaltasy remains as a new
789 species of *Rectia*. *Rectia magna* is probably the remains of eukaryotic filamentous
790 microorganisms (Fig. 10). Some *Rectia* specimens superficially resemble the tightly coiled
791 filaments of *Obruchevella* or *Spiromorpha*, but the bispiral pattern observed in these genera
792 is not traceable in the tubes with prominent doubled annulations. Nor does it appear that the
793 annulations originated as tubes rather than as reinforced sheets.

794

795 *Rectia magna* Sergeev, Knoll and Vorob'eva new species
796 Figures 6.1-6.6
797 *Botuobia* spp.: Veis et al., 2000, pl. 2, Figs. 9, 11, 13 and 20.
798 Ex gr. *Botuobia*: Veis et al., 2000, pl. 3, Fig. 5.
799 *Diagnosis*: A species of *Rectia* with cross-sectional diameter 70-200 µm.
800 *Description*: Compressed, unbranched tubes tapering sharply at its terminus, with prominent
801 doubled annulations separated by thin-walled intervals. Cross sectional diameter 70-200 µm
802 (n = 7, µ= 132µm, σ = 43, RSD = 32.5%); tubes up to 250 µm long (incomplete specimens);
803 tube walls translucent, medium-grained, ca. 1-2 µm thick. Pseudocellular, opaque, granulated,
804 double annulations 3.0-10.5 µm wide (n = 37, µ= 6.5µm, σ = 2.3, RSD = 35%) and possibly
805 2-3 µm high with intervening areas 1.5-3.5 µm and 0.5-2.0 µm wide between doubled
806 annulations and within pairs of annulations (when visible), respectively.
807 *Etymology*: From Latin *magna* – large, great, with reference to the taxon's large size
808 compared with previously described species of *Rectia*.
809 *Type*: Figure 6.3, GINPC 14712-5408, borehole 133 Azino-Pal'nikovo, 2052 m depth (See
810 Veis et al., 2000, pl. 3, Fig. 5).
811 *Material examined*: Seven well-preserved and additionally poorly preserved specimens.

Occurrence: Lower Mesoproterozoic, Kaltasy Formation, Cis-Urals area, East European Platform.

Remarks: *Rectia magna* is closely similar to *R. costata* Yankauskas (1980) in morphology and, in principle, the two could reflect a single biological entity. Two considerations prompt us to diagnose a new species of *Rectia*: the ages of the Kaltasy *Rectia* and *R. costata* do not overlap (500 million year difference), and the size distributions of the two populations do not overlap (70-200 µm for *R. magna* vs. 35 µm for *R. costata*). These considerations are challenging for the hypothesis of biological uniformity, and so we prefer keep these species separate, following common practice in paleobotany.

Genus *Rugosoopsis* Timofeev and Hermann, 1979

Type species: *Rugosoopsis tenuis* Timofeev and Hermann, 1979

Rugosoopsis sp.

Figures 6.11, 6.12

Rugosoopsis sp.: Sperling et al., 2014, Fig. 4.13.

Description: Compressed, unbranched rigid tubes containing numerous cross-ribs. Tubes 45-350 µm in cross-sectional diameter (significantly large variance) and up to 550 µm long (incomplete specimen); tube walls translucent, medium-grained, ca. 1-2 µm thick. Ribs opaque, 1-2 µm wide; distance between ribs ranges from 6-10 to 20 µm.

Material examined: Two moderately well preserved specimens.

Remarks: This form differs from *R. tenuis* in its larger tube and thinner wall. Therefore, we have chosen to identify this form as *Rugosoopsis* sp.

7.4. Filamentous microfossils

Genus *Cephalonyx* A. Weiss, in Veis, 1984 emend. Butterfield, in Butterfield et al., 1994

Type species: *Cephalonyx coriaceus* (Asseeva) (in Asseeva and Velikanov, 1983)

838 *Cephalonyx* sp.

839 Figures 7.4 and 7.8

840 *Oscillatoriopsis* spp.: Veis et al., 2000, pl. 2, Fig. 8.

841 *Description*: Unbranched tubes with prominent doubled annulations separated by thin-walled
842 intervals. Pseudocellular opaque granulated annulations 25-50 μm wide and 5-10 μm long
843 tapering toward apices to 9-14 μm and separated by translucent intervening areas 2.5-4.5 μm
844 long. Length of tube is about 100 μm (incomplete specimen preserved).
845 *Remarks*: Here we follow the emended diagnosis of genus *Cephalonyx* suggested by
846 Butterfield in Butterfield et al., 1994, who interpreted these fossils as pseudocellular fossil
847 sheaths. It may be that some specimens interpreted as sheaths are in fact compressed
848 ensheathed trichomes in which cross walls have been lost (Golubic and Barghoorn, 1977;
849 Gerasimenko and Krylov, 1983; Hofmann and Jackson, 1994; Sergeev et al., 1995);
850 however, the Kaltasy population exhibits features best interpreted in terms of pseudocellular
851 sheaths, especially the ripped ends of preserved filaments, where irregular edges cut across
852 cell-like features (Fig. 7.8). This is expected if the fossils are sheaths, unexpected it they were
853 actually trichomes. [See also *Cephalonyx* as, described by Veis (1984), which tapers toward
854 apices and has large discoidal and S-like cell shapes probably preserved as casts with
855 cyanobacterial sheaths.] Tapering toward apices may be original, but can also reflect *post-*
856 *mortem* shrinkage of filaments (Golubic and Barghoorn, 1977; Gerasimenko and Krylov,
857 1983; Sergeev, 1992; Knoll and Golubic, 1992). In its morphometric characteristics
858 *Cephalonyx* sp. resembles *Cephalonyx sibiricus* A.Weiss (in Veis, 1984), but in general is
859 smaller.
860 *Material examined*: Two moderately well-preserved specimens.
861

862 Genus *Polytrichoides* Hermann, 1974, emend. Hermann, in Timofeev et al., 1976
863 *Type species*: *Polytrichoides lineatus* Hermann, 1974

Polytrichoides aff. *P. lineatus* Hermann, 1974, emend. Hermann in Timofeev et al., 1976

Figure 7.1

Polytrichoides lineatus Hermann, 1974, p. 8, pl. 6, Figs. 3 and 4; Timofeev et al., 1976, p. 37, pl. 14, Fig. 7; Yankauskas, 1989, p.119-120, pl. 30, Figs. 5a, 5б, 6, and 7; Hermann, 1990, pl. 9, Figs. 8 and 8a; Schopf, 1992, pl. 27, Figs. A_1 and A_2; Gnilovskaya et al., 2000, pl. 2, Figs. 16 and 17; Veis and Petrov, 1994a, pl. 2, Figs. 25 and 27; Vorob'eva et al., 2006, Fig. 2e; Vorob'eva et al., 2009, p.188, Figs.15.13 and 15.14; Sergeev et al., 2012, p. 342, pl. 29, Figs. 6-8; Tang et al., 2013, p. 178, Fig. 14; Vorob'eva et al., 2015, p. 218, Figs. 9.5 and 9.7-9.11.

Majaphyton antiquam Timofeev and Hermann, 1979 (partim): Veis et al., 2000, pl. 3, Fig. 14.

Non *Polytrichoides lineatus*: Veis et al., 2000, pl. 2, Figs. 14 and 15 (For additional synonymy see Sergeev et al., 2012 and Tang et al., 2013).

Description: Bundles of tubular structures closely grouped within a common cylindrical sheath that tapers toward ends. Tubular structures1.5-4.5 μm in diameter, walls translucent, hyaline, 0.5-1.0 thick. The surrounding sheath is cylindrical, commonly tapering toward both closed and open ends, 25-45 μm wide and up to 350 μm long. Sheath walls translucent, hyaline or fine grained, 1-2 μm thick.

Material examined: A few poorly preserved specimens.

Occurrence: Widely distributed in Proterozoic microfossil assemblages.

Remarks: Like the broadly similar taxa *Eoschizothrix* Lee Seong-Joo and Golubic, 1998 and *Eomicrocoleus* Horodyski and Donaldson 1980, filaments of *Polytrichoides* are commonly compared with the modern polytrichomous hormogonian cyanobacteria *Microcoleus*, *Hydrocoleum* or *Schizothrix* (See Sergeev et al., 2012).

Genus *Pseudodendron* Butterfield, in Butterfield et al., 1994

Type species: *Pseudodendron anteridium* Butterfield (in Butterfield et al., 1994).

Pseudodendron anteridium Butterfield, in Butterfield et al., 1994

Figures 8.1 – 8.3

Pseudodendron anteridium Butterfield, in Butterfield et al., 1994, p. 70, 72, Figs. 28A-28G, and 28J; Butterfield, 2009, Figs. 3A and 3B; Vorob'eva et al., 2015, p. 218, 219, Figs. 9.1-9.4.

A broad filamentous sheath: Veis and Vorob'eva, 1992, pl. 1, Figs. 12, 15, and 20; Veis and Petrov, 1994a, pl. 3, Fig. 5; Veis et al., 2001, Fig. 2o.

A branching filament: Veis and Petrov, 1994a, pl. 3, Fig. 22.

Archaeoclada sp.: Veis et al., 2000, pl. 3, Figs. 16 and 17.

Pseudodendron aff. *P. anteridium:* Sperling et al., 2014, Fig. 4.11

Description: Heterogeneous branching thalli sometime tapering toward apices with an outer sheath and terminal expansion. Branching is lateral or dichotomous, and two levels of branching are clearly present. Thalli are translucent to opaque, with spumose texture. Sheath translucent but not always visible; conspicuous at branch junctions where the sheath can occur on the inside angle as a prominent subtriangular gusset. Thalli 25-125 μm in cross-sectional diameter, up to 1000 μm long (incomplete specimen); sheath wall medium-grained, ca. 1-2 μm thick.

Material examined: Approximately fifty well-preserved specimens.

Occurrence: Widely distributed in Proterozoic microfossil assemblages.

Remarks: This form is compared with either branching filaments of cyanobacteria (Butterfield et al., 1994) or eukaryotic algae.

Genus *Siphonophycus* Schopf, 1968, emend. Knoll and Golubic, 1979, emend. Knoll et al., 1991

Type species: *Siphonophycus kestron* Schopf, 1968.

Siphonophycus punctatum Maithy, 1975, emend. Buick and Knoll, 1999

Figure 8.7

Siphonophycus punctatus Maithy, 1975, p. 137, pl. 1, Fig. 5.

Siphonophycus punctatum Buick and Knoll, 1999, p. 761, Figs. 6.2-6.4 and 6.6.

Asperatofilum experatus Hermann, in Yankauskas, 1989, p. 100, pl. 26, Fig. 16; Veis and Petrov, 1994a, pl. 1, Figs. 25 and 26, pl. 2, Fig. 26, pl. 3, Fig. 17; Veis et al., 2000, pl. 2, Figs. 5, 7, 17 and 21 (for additional synonymy see Buick and Knoll, 1999).

Description: Unbranched solitary nonseptate tubes, cylindrical to slightly compressed and 32.0 to 64.0 μm broad, that rarely contain degraded trichomic thread-like amorphous fragments; tube walls range from smooth to fine-or medium-grained, 0.5 to 1.0 thick.

Occurrence: Widely distributed in Proterozoic microfossil assemblages.

Material examined: About a hundred well-preserved specimens.

Genus *Tortunema* Hermann, in Timofeev et al., 1976, emend. Butterfield, in Butterfield et al., 1994

Type species: Tortunema Wernadskii (Schepeleva,1960)

Tortunema patomica (Kolosov,1982), emend. and comb. Butterfield (in Butterfield *et al.*, 1994)

Figures 7.3 and 7.5

Palaeolyngbya patomica Kolosov, 1982, p. 72, pl. 10, Fig. 1.

Botuobia patomica Kolosov, 1984, p. 48-49, pl. 9, Fig. 2; Yankauskas, 1989, p. 101, pl. 43, fig. 3.

Botuobia angustata Kolosov, 1984, p. 49-50, pl. 10, Fig. 1.

Botuobia diversa Kolosov, 1984, p. 50, pl. 11, Fig. 1.

Palaeolyngbya sphaerocephala Hermann and Pylina in Hermann, 1986 (partim): Veis et al., 2000, pl. 2, Fig. 6.

Description: Unbranched solitary cylindrical compressed tubes 45 to 50 μm broad (20 μm in narrowest part) and tapering toward both ends; contains degraded opaque thread-like fragments 10-15 μm wide. Tubes transparent or translucent, prominent, non-lamellated, about 0.5 μm thick and up to 400 μm long with clear annular lines 1-2 μm long separated by intervening regions 5-7 μm long.

Material examined: One well-preserved and a few medium to poorly preserved specimens.

944 *Age and distribution:* Mesoproterozoic: Kaltasy Formation, 203 Bedryazh and 133 Azino-
945 Pal'nikovo boreholes; Ediacaran, Kursov Formation, Siberia.
946 *Remarks*: *Tortunema* was originally erected to describe septate (pseudoseptate) sheaths that
947 taper toward both ends. We follow here the formal classification of Butterfield in
948 Butterfield et al., 1994, accepting *Botuobia* as a junior synonym of *Tortunema* and
949 separating the latter into species on the basis of tube diameter, much like the convention for
950 *Siphonophycus* sheaths (Butterfield et al., 1994, p. 69). Although generally interpreted as
951 pseudosepatate sheaths, *Tortunema* might alternatively be considered trichomes which lost
952 septa during diagenesis. This interpretation is unlikely for the Kaltasy population, both
953 because ripped ends cut across "septa" (Fig. 7.3; see discussion of *Cephalonyx)* and
954 because some specimens contain remnants of shrunken cells (Fig. 7.5), obviating
955 interpretation of the entire specimen as a trichome.
956
957 7.5. *Miscellaneous microfossils*
958 Genus *Pellicularia* Yankauskas, 1980
959 Type species: *Pellicularia tenera* Yankauskas, 1980
960 *Pellicularia tenera* Yankauskas, 1980
961 Figures 8.8, 8.9 and 8.10
962 *Pellicularia tenera* Yankauskas, 1980, p. 110, pl. 12, Fig. 9; Yankauskas, 1989, p. 139, pl. 42, Figs. 3-5; Veis
963 et al., 2000, pl. 3, Fig. 6.
964 *Description*: Fusiform-like and ribbon-like structures 25-70 µm across and up to 350 µm
965 long, with longitudinal intertwined thread-like filaments 1-2 µm in diameter incorporated
966 inside the main body. Walls translucent, about 1 µm thick, with folds 1-2 µm wide; surface
967 granular to shagrinate.
968 *Remarks*: Yankauskas (1980) described this taxon from the Neoproterozoic (Upper
969 Riphean) Schtanda Formation of Cis-Urals area, but his treatment has not been broadly

recognized. Veis et al. (2000) described it from the Kaltasy Formation, using this to argue for a Neoproterozoic age. The affinities of the microfossils are uncertain.

Material examined: Four well-preserved specimens.

Age and distribution: Mesoproterozoic: Kaltasy Formation, 203 Bedryazh and 133 Azino-Pal'nikovo boreholes; Neoproterozoic: Schtanda Formation, 62 Kabakovo borehole, Cis-Urals area, East European Platform.

Unnamed Form 1

Figures 9.1, 9.2 and 9.3

Description: Translucent irregular ellipsoidal or elongated vesicles arranged in clusters from a few individuals joined each other by their walls. Vesicles 100-265 µm across and 240-390 µm long; surface reticulated, with a granulated wall 1.0-1.5 µm thick.

Material examined: Five well-preserved specimens.

Remarks: Unnamed Form 1 exhibits a reticulated surface that could reflect *post-mortem* alteration. Clusters of vesicles could also formed by secondary aggregation of the dead cells. Originally, therefore, these microorganisms could have been smooth-walled vesicles similar to *Leiosphaeridia*. Given the large uncertainties in basic interpretation, we prefer to describe it informally, noting only that it contributes to the overall diversity recorded by the Kaltasy assemblage.

Unnamed Form 2

Figures 9.4, 9.5 and 9.6

Envelopes with problematic spines or pseudospines: Sperling et al., 2014, Fig. 4.5.

Description: Solitary, translucent to opaque vesicles of spherical and subspherical shape 150-785 µm across, but irregular in outlines. Vesicles bear blunt conical and elongated spine-like structures 40-130 µm wide (near base) and 15-65 µm long. Walls translucent,

996 medium-grained, 1.0-2.0 μm thick and sometime are surrounded by outer translucent
997 membrane about 0.5 μm thick.
998 *Material examined*: Five relatively poorly preserved specimens.
999 *Remarks*: The origin of spine-like structures that cover the vesicle surface is uncertain;
1000 given their irregular shape, we suspect that these originated during diagenesis.
1001
1002 Unnamed Form 3
1003 Figures 9.7 and 9.10
1004 *Description*: Solitary, single-layered translucent spheroidal or ellipsoidal vesicles with
1005 rounded ends. Vesicle surface is covered with small spine-like structures sometimes
1006 surrounded by a halo- or membrane-like transparent structure. Vesicle diameter 35-100
1007 μm; walls translucent, medium-grained, less than 1 μm thick; spine-like structures 1.5-5
1008 μm wide and 2-4 μm long.
1009 *Material examined*: Twenty three variously preserved specimens.
1010 *Remarks*: The genesis of spine-like structures covering surfaces of Unnamed Form 3 is
1011 uncertain. They are probably of secondary origin, similar to many pseudospines
1012 observed on originally smooth surfaces of cyanobacteria (e.g., Sergeev et al., 1995,
1013 Fig. 7.10; 2012, pl. 7, Figs. 8-10, pl. 27, Fig. 5; Sergeev, 2006, pl. 1, Fig. 10, pl. 21,
1014 Figs. 10-13, pl. 23, Figs. 1-8). However, as in all previous cases (Unnamed Forms 1 and
1015 2) we cannot rule out an option that these structures are of primarily origin and so describe
1016 them here only informally.
1017
1018 Unnamed Form 4
1019 Figures 9.8, 9.9, 9.11 and 9.12
1020 Paired envelopes of *Leiosphaeridia jacutica*: Sperling et al., 2014, Fig. 4.9

Description: Elongated translucent to opaque vesicles, solitary, in pairs, or arranged in *an echelon* style 2 or 3 together. Vesicles translucent to opaque 100-350 µm wide and 180-500 µm long, with wall up to 2 µm thick (when visible), with a shagrinate surface and typically a system of perpendicular cracks or transverse annulations 1-3 µm wide in the equatorial regions.

Remarks: These microfossils resemble microfossils recently described from Neoproterozoic deposits of China as *Pololeptus rugosus* (Tang et al., 2013). Similarities, however, could reflect diagenetic convergence.

Material examined: Twenty well-preserved specimens.

Unnamed Form 5

Figures 9.13 and 9.14

Description: Elongated translucent solitary vesicles composed of two or three segments that communicate freely each to other, but with constrictions at conjunctions. Some vesicles exhibit elongated, blunt, horn-like protrusions. Vesicle surface fine-grained and covered with small dark irregular grains. Vesicle width 100-700 µm, length 135-815 µm; protrusions 10-15 µm wide and 15-20 µm long; walls 0.5-1.0 µm thick.

Material examined: Eight variously preserved specimens.

Remarks: The morphology of the microfossils is quite unusual for Proterozoic microfossils. Upon recovery of better preserved samples, this population could deserve recognition as a new genus, but given the quality of our specimens and lingering uncertainty about diagenetic alteration, we describe it here only informally.

Acknowledgements.

1045 We thank the late V.I. Kozlov, who facilitated this research and Heda Agić and an
1046 anonymous reviewer for comments that materially improved our paper. We also thank the
1047 NASA Astrobiology Institute (AHK) and RFBR Grants 13-05-00127, 14-05-00323 and the
1048 Program of the Presidium of Russian Academy of Sciences 30 (VNS and NGV) for
1049 research support.

1050 References

1051

1052 Adam, Z.R., 2014. Microfossil Paleontology and Biostratigraphy of the Early
1053 Mesoproterozoic Belt Supergroup, Montana. Unpublished Ph.D. thesis, Montana
1054 State University.
1055 Agić, H., Moczydłowska, M., Yin, L., 2015. Affinity, life cycle, and intracellular
1056 complexity of organic-walled microfossils from the Mesoproterozoic of Shanxi,
1057 China. Journal of Paleontology 89, 28-50.
1058 Anbar, A.D., Knoll, A.H., 2002. Proterozoic ocean chemistry and evolution: a bioinorganic
1059 bridge? Science 297, 1137-1142.
1060 Asseeva, E.A., Velikanov, V.A., 1983. New finds of the fossilized plant remains in the
1061 Vendian Layadovskaya layers of Podolia (Upper Precambrian), in: Fossil fauna and
1062 flora of Ukraine. Naukova Dumka, Kiev, pp. 3-8 (In Russian).
1063 Bartley, J. K., 1996. Actualistic taphonomy of cyanobacteria: implications for the
1064 Precambrian fossil record. Palaios 11, 571-586.
1065 Becker, B., 2013. Snow ball Earth and the split of Streptophyta and Chlorophyta. Trends in
1066 Plant Science 18, 180-183.
1067 Bhattacharya, S., Dutta, S., 2015. Neoproterozoic-Early Cambrian biota and ancient niche:
1068 A synthesis from molecular markers and palynomorphs from Bikaner-Nagaur
1069 Basin, western India. Precambrian Research 266, 361-374.
1070 Brotzen, F., 1941. Några bidrag till visingsöformationens stratigrafi och tektonik. Geologiska
1071 Foreningens Forhandlingar 63, 245-261.

1072 Buick, R., Knoll, A.H., 1999. Acritarchs and microfossils from the Mesoproterozoic
1073 Bangemall Group, Northwestern Australia. Journal of Paleontology 73, 744-764.

1074 Butterfield, N.J., 2009. Modes of pre-Ediacaran multicellularity. Precambrian Research
1075 173, 201-211.
1076 Butterfield, N.J., Chandler, F.W., 1992. Paleoenvironmental distribution of Proterozoic
1077 microfossils, with an example from the Agu Bay Formation, Baffin Island.
1078 Palaeontology 35, 943–957.

1079 Butterfield, N.J., Knoll, A.H., Swett, K., 1994. Paleobiology of the Neoproterozoic
1080 Svanbergfjellet Formation, Spitsbergen. Fossils and Strata 34, 1-84.
1081 Combaz, A., Lange, F.W., Pansart, J., 1967. Les ‘‘Leiofusidae’’ Eisenack, 1938. Review
1082 of Palaeobotany and Palynology 1, 207–307.
1083 Cramer, F.H., 1970. Distribution of selected Silurian acritarchs; an account of the
1084 palynostratigraphy and paleogeography of selected Silurian acritarch taxa. Revista
1085 Espanola de Micropaleontologia (numero extraordinario), 1-203, pis I-XXIII.
1086 Chumakov, N.M., Semikhatov, M.A. 1981. Riphean and Vendian of the USSR.
1087 Precambrian Research 15, 229–253.
1088 Deunff, J., 1955. Un microplancton fossile Dévonien a Hystrichosphéres du Continent
1089 Nord–Américain. Bulletin de la Microscopie Appliqué, Séries 2, 5, 138–149.
1090 Downie, C., Sarjeant, W.A.S., 1963. On the interpretation and status of some
1091 Hystrichosphere genera. Palaeontolgy 6, 83-96.
1092 Eisenack, A., 1958. Microfossilien aus dem Ordovizium des Baltikums. 1. Markasitschicht,
1093 Dictyonema-Scheifer, Glaukonitsand, Glaukonitkalk. Senckenbergian Lethaea 39,
1094 389–404.
1095 Elenkin, A.A., 1949. Monographia algarum Cyanophycearum aquidulcium et terrestrium in
1096 finibus URSS inventarum. Pars specialis (Systematica), Fasc. II. III. Hormogoneae
1097 (Geitl.) Elenk. Sumptibus Academiae Scientarum URSS, Moscow and Leningrad,
1098 pp. 985-1908 (In Russian).

1099 Eme, L., Sharpe, S.C., Brown, M.W., Roger, A.W., 2014. On the age of eukaryotes:
1100 Evaluating evidence from fossils and molecular clocks. Cold Spring Harbor
1101 Perspectives in Biology, doi: 10.1101/cshperspect.a016139.
1102 Fairchild, T.R., 1985. Size as a criterion for distinguishing probable eukaryotic unicells in
1103 silicified Precambrian microfloras. 8th Congresso Brasileiro de Paleontologia, Rio
1104 de Janeiro. Sociedade Brasileira de Paleontologia. Anais (MME-DNPM. Sèrie
1105 Geologia n. 27), pp. 1-8.
1106 Ford, T.D., Breed, W., 1973. The problematical Precambrian fossil *Chuaria*. Palaeontology
1107 16, 535-550.
1108 Gerasimenko, L.M., Krylov, I.N., 1983. Post-Mortem changes in cyanobacteria from the
1109 algal-bacterial mats of thermal springs. Doklady Akademii Nauk SSSR 172(1),
1110 201–203 (In Russian).
1111 Giovannoni, S.J., Turner, S., Olsen, G.J., Barns, S., Lane, D.J., Pace, N.R., 1988.
1112 Evolutionary relationships among cyanobacteria and green chloroplasts. Journal of
1113 Bacteriology 170, 3584-3592.
1114 Gnilovskaya, M.B., Veis, A.F., Bekker, Y.R., Olovyanishnikov, V.G., Raaben, M.E., 2000.
1115 Pre-Ediacaran fauna from Timan (Annelidomorphs of the Late Riphean).
1116 Stratigraphy and Geological Correlation 8, 11-39.
1117 Golubic, S., Barghoorn, E.S., 1977. Interpretation of microbial fossils with special
1118 reference to the Precambrian, in: Flügel, E. (Ed.), Fossil algae. Berlin-Heidelberg-
1119 N.Y., Springer-Verlag, pp. 1–14.
1120 Golubic, S., Sergeev, V.N., Knoll, A.H., 1995. Mesoproterozoic *Archaeoellipsoides*:
1121 akinetes of heterocystous cyanobacteria. Lethaia 28, 285–298.
1122 Gorozhanin, V.M., 1995. Candidate's Dissertation in Geology and Mineralogy
1123 (Yekaterinburg, 1995).

1124 Gray, J., Boucot, A.J., 1989. Is *Moyeria* a euglenoid? Lethaia 22, 447–456. DOI
1125 10.1111/j.1502-3931.1989.tb01449.x
1126 Grey, K., 1999. A modified palynological preparation technique for the extraction of large
1127 Neoproterozoic acanthomorphic acritarchs and other acid insoluble microfossils.
1128 Gelogical Survey of Western Australia Record 10, 1-23.
1129 Grey, K., 2005. Ediacaran palynology of Australia. Memoir of the Association of
1130 Australasian Palaeontologists 31, 1-439.
1131 Guilbaud, R., Poulton, S.W., Butterfield, N.J., Zhu, M.Y., Shields-Zhou, G.A., 2015. A
1132 global transition to ferruginous conditions in the early Neoproterozoic oceans.
1133 Nature Geoscience 8, 466-468.
1134 Le Hérissé, A., Paris, F., Steemans, P., 2013. Late Ordovician–earliest Silurian
1135 palynomorphs from northern Chad and correlation with contemporaneous deposits
1136 of southeastern Libya. Bulletin of Geosciences 88(3), 483–504.
1137 Hermann, T.N., 1974. Finds of massive accumulations of trichomes in the Riphean, in:
1138 Timofeev, B.V. (Ed.), Microfossils of Proterozoic and early Paleozoic of the USSR.
1139 Nauka, Leningrad, pp. 6-10 (In Russian).
1140 Hermann, T.N., 1986. The finds of filamentous blue-green algae in the Upper Precambrian
1141 (the Miroedikha Formation), in: Actual problems of modern paleoalgology.
1142 Naukova Dumka, Kiev, pp. 37-40 (In Russian).
1143 Hermann, T.N., 1990. Organic world a billion years ago. Nauka, Leningrad (In Russian,
1144 with English summary).
1145 Hermann, T.N., Podkovyrov, V.N., 2009. New insights into the nature of the Late Riphean
1146 *Eosolenides*. Precambrian Research 173, 154-162.
1147 Hermann, T.N., Podkovyrov, V.N., 2014. Formation of an unusual form of Riphean
1148 *Eosolenides*. Paleontological Journal 48, 345–352.

1149 Hermann, T.N., Timofeev, B.V., 1985. *Eosolenides*, a new group of problematic
1150 organisms from the Late Precambrian, in: Problematics of the Late Precambrian and
1151 Paleozoic. Nauka, Novosibirsk, pp. 9-15 (In Russian).
1152 Hofmann, H.J., Jackson, G.D., 1994. Shale-facies microfossils from the Proterozoic Bylot
1153 Supergroup, Baffin Island, Canada. Palaeontological Society Memoir 37, 1-39.
1154 Horodyski, R.J., Donaldson, J.A., 1980. Microfossils from the Middle Proterozoic Dismal
1155 Lakes Group, Arctic Canada. Precambrian Research 11, 125-159.
1156 Ishida, T., Watanabe M.K., Sugiyama J., Yokota, A., 2001. Evidence for polyphyletic
1157 origin of the members of the orders of Oscillatoriales and Pleurocapsales as
1158 determined by 16S rDNA analysis. FEMS Microbiology Letters 201, 79-82.
1159 Javaux, E.J., Knoll, A.H., Walter, M.R., 2001. Morphology and ecological complexity in
1160 early eukaryotic ecosystems. Nature 412 (6872), 66–69.
1161 Javaux, E.J., Knoll, A.H., Walter, M.R., 2004. TEM evidence for eukaryotic diversity in
1162 mid-Proterozoic oceans. Geobiology 2, 121–132.
1163 Johnston, D.T, Wolfe-Simon, F., Pearson, A., Knoll. A.H., 2009. Anoxygenic
1164 photosynthesis modulated Proterozoic oxygen and sustained Earth's middle age.
1165 Proceedings of the National Academy of Sciences, USA 106, 16925–16929.
1166 Kah, L.C., Crawford, D.C., Bartley, J.K., Kozlov, V.I., Sergeeva, N.D., Puchkov, V.N.
1167 2007. C- and Sr-isotope chemostratigraphy as a tool for verifying age of Riphean
1168 deposits in the Kama-Belaya Aulacogen, the East European Platform. Stratigraphy
1169 and Geological Correlation 15, 12–29.
1170 Keller, B.M., Chumakov, N.M. (Eds.), 1983. Stratotype of the Riphean, Stratigraphy,
1171 Geochronology. Nauka, Moscow (In Russian).
1172 Knoll, A.H., 1984. Microbiotas of the Late Precambrian Hunnberg Formation,
1173 Nordaustlandet, Svalbard. Journal of Paleontology 58, 131–162.

1174 Knoll, A.H., Golubic, S., 1979. Anatomy and taphonomy of a Precambrian algal
1175 stromatolite. Precambrian Research 10, 115–151.
1176 Knoll, A.H., Golubic, S., 1992. Living and Proterozoic cyanobacteria, in: Schidlowski, M.,
1177 et al. (Eds.), Early organic evolution: Implication for mineral and energy resources.
1178 Springer-Verlag, Berlin, pp. 450–462.
1179 Knoll, A.H., Sergeev, V.N., 1995. Taphonomic and evolutionary changes across the
1180 Mesoproterozoic-Neoproterozoic transition. Neues Jabrbuch für Geologie und
1181 Paläontologie Abhandlungen 195 (1/3), 289-302.
1182 Knoll, A.H., Sweet, K., Mark, J., 1991. Paleobiology of a Neoproterozoic tidal
1183 flat/lagoonal complex: the Draken Conglomerate Formation, Spitsbergen. Journal
1184 of Paleontology 65, 531-570.
1185 Knoll, A.H., Summons, R.E., Waldbauer, J., Zumberge, J., 2007. The geological
1186 succession of primary producers in the oceans, in: Falkowski, P., Knoll, A.H.
1187 (Eds.), The evolution of primary producers in the sea. Elsevier, Burlington, pp. 133-
1188 163.
1189 Kodner, R.B., Summons, R.E., Pearson, A., Knoll, A.H., 2008. Sterols in red and green
1190 algae: quantification, phylogeny and relevance for the interpretation of geologic
1191 steranes. Geobiology 6, 411-420.
1192 Kolosov, P.N., 1982. Upper Precambrian paleoalgological residues from the Siberian
1193 Platform. Nauka, Moscow (In Russian).
1194 Kolosov, P.N., 1984. Late Precambrian microorganisms from the Eastern Siberian Platform.
1195 Yakutskii Filial AN SSSR, Yakutsk (In Russian).
1196 Kozlov, V.I., Muslimov, R. Kh., Gatiyatullin, N.S. et al., 1995. Upper Precambrian of
1197 Eastern Tatarstan: Implications for Oil and Gas Prospecting. Institute of Geology,
1198 Ufa (in Russian).

1199 Kozlov, V.I., Sergeeva, N.D., 2011. Upper Proterozoic of the Volgo-Ural region.
1200 Stratigraphy and composition, Geology. Proceedings on the Earth Sciences and
1201 Mineral Resources of the Academy of Sciences of Bashkirian Republic 17, 58–80
1202 (In Russian).
1203 Kozlov, V.I., Sergeeva, N.D., Mikhailov, P.N., 2009. Stratgraphic subdivision of the
1204 boundary Upper Riphean, Vendian and Paleozoic deposits of western
1205 Bashkortostan. Bulletin of the Regional Interdepartmental Stratigraphic
1206 Commission on the Central and Southern Parts of the Russian Plate 4, 40–44 (In
1207 Russian).
1208 Kozlov, V.I., Puchkov, V.N., Sergeeva, N.D., 2011. New Chart of Geological Succession
1209 Revealed by the Parametric Borehole 1 Kulguninskaya. Institute of Geology, Ufa,
1210 (In Russian).
1211 Krasnobaev, A., Kozlov, V.I., Puchkov, V.N., Busharina, S.V., Sergeeva, N.D., Paderin,
1212 I.P., 2013a. Zircon geochronology of the Mashak volcanic rocks and the problem of
1213 the age of the lower-middle Riphean boundary (Southern Urals). Stratigraphy and
1214 Geological Correlation 21, 465–481.
1215 Krasnobaev, A.A., Puchkov, V.N., Kozlov, V.I., Sergeeva, N.D., Busharina, S.V.,
1216 Lepekhina, E.N., 2013b. Zirconology of Navysh volcanic rocks of the Ai suite and
1217 the problem of the age of the Lower Riphean boundary in the Southern Urals.
1218 Doklady Earth Sciences 448, 185-190.
1219 Kumar, S., Srivastava, P., 1995. Microfossils from the Kheinjua Formation,
1220 Mesoproterozoic Semri Group, Newari area, central India. Precambrian Research
1221 74,91-117
1222 Lee Seong-Joo, Golubic, S., 1998. Multi-trichomous cyanobacterial microfossils from the
1223 Mesoproterozoic Gaoyuzhuang Formation, China: Paleontological and taxonomic
1224 implications. Lethaia 31,169-184.

1225 Littler, M.M., Littler D.S, Blair, S.M. Norris, J.N., 1985. Deepest known plant life
1226 discovered on an uncharted seamount. Science 227, 57-59.
1227 Mädler, K., 1964. Bemerkenswerte Sporenformen aus dem Keuper und unteren Lias.
1228 Fortschritte in der Geologie von Rheinland and Westfalen 12, 169-170.
1229 Maithy, P.K., 1975. Micro-organisms from the Bushimay System (Late Precambrian) of
1230 Kanshi, Zaire. Palaeobotanist 22,133-149.
1231 Margulis, L., Grosovski, B.D.D., Stolz, J.F., Gong-Collins, E.J., Lenk, S., Read, D., Lopèz-
1232 Cortès, A., 1983. Distinctive microbial structure and the pre-Phanerozoic fossil
1233 record. Precambrian Research 20, 443–478.
1234 Margulis, L., Corliss, J.O., Melkonnian, M. Chapman, D.J. (eds.), 1990. Handbook of
1235 Protoctista. Jones and Barlett, Boston.
1236 Miller, A., Eames, L., 1982. Palynomorphs from the Silurian Medina Group (Lower
1237 Llandovery) of the Niagara Gorge, Lewiston, New York, U.S.A. Palynology 6,
1238 221–254.
1239 Moczydłowska, M., 2008. New records of late Ediacaran microbiota from Poland.
1240 Precambrian Research 167, 71-92.
1241 Moczydłowska, M., 2010. Life cycle of Early Cambrian microalgae from the *Skiagia*-
1242 plexus acritarchs. Journal of Paleontology 84, 216-230.
1243 Moczydłowska, M., 2015. Algal affinities of the Ediacaran and Cambrian organic-walled
1244 microfossils with internal reproductive bodies: *Tanarium* and other morphotypes.
1245 Palynology 40, 83-121 doi: 10.1080/01916122.2015.1006341.
1246 Moczydłowska, M., Schopf, J.W., Willman, S., 2010. Micro- and nano-scale ultrastructure
1247 of cell walls in Cryogenian microfossils: revealing their biological affinity. Lethaia
1248 43, 129-136.
1249 Moczydłowska, M., Landing, E., Zhang, W., Palacios, T., 2011. Proterozoic phytoplankton
1250 and timing of chlorophyte algae origin. Palaeontology 54, 721–733.

1251 Molyneux, S.G., Barron, H.F., Smith R.A., 2008. Upper Llandovery-Wenlock (Silurian)
1252 palynology of the Pentland Hills inliers, Midland Valley of Scotland. Scottish
1253 Journal of Geology 44, 151-168.
1254 Nagovitsin, K., 2009. *Tappania*-bearing association of the Siberian platform: Biodiversity,
1255 stratigraphic position and geochronological constraints. Precambrian Research 173,
1256 137-145.
1257 Pang, K., Tang, Q., Schiffbauer, J.D., Yao, J., Yuan, X., Wan, B., Chen, L., Ou, Z., Xiao,
1258 S., 2013. The nature and origin of nucleus-like intracellular inclusions in
1259 Paleoproterozoic eukaryote microfossils. Geobiology 11, 499–510.
1260 Pang, K., Tang, Q., Yuan, X., Wan, B., Xiao, S., 2015. A biomechanical analysis of the
1261 early eukaryotic fossil *Valeria* and new occurrence of organic-walled microfossils
1262 from the Paleo-Mesoproterozoic Ruyang Group. Palaeoworld 24, 251–262.
1263 Parfrey, L., Lahr, D., Knoll, A.H., Katz, L.A., 2011. Estimating the timing of early
1264 eukaryotic diversification with multigene molecular clocks. Proceedings of the
1265 National Academy of Sciences, USA 108, 13624–13629.
1266 Peat, C.J., Muir, M.D., Plumb, K.A., McKirdy, D.M., Norvick, M.S., 1978. Proterozoic
1267 microfossils from the Roper Group, Northern Territory, Australia. BMR Journal of
1268 Australian Geology and Geophysics 3, 1-17.
1269 Petrov, P.Yu., Veis, A.F., 1995. Facial-ecological structure of the Derevnya Formation
1270 microbiota: Upper Riphean, Turukhansk Uplift, Siberia. Stratigraphy and
1271 Geological Correlation 3, 18-51.
1272 Prasad, B., Asher, R. 2001. Biostratigraphy and lithostratigraphic classification of
1273 Proterozoic and Lower Paleozoic sediments (Pre-Unconformity Sequence) of
1274 Ganga Basin, India. Paleontographica Indica 5, 1-151.

1275 Prasad, B., Uniyal, S.N., Asher, R., 2005. Organic walled microfossils from the Proterozoic
1276 Vindhyan Supergroup of Son Valley, Madhya Pradesh, India. Palaeobotanist 54,
1277 13-60.
1278 Puchkov, V.N., 2005. Evolution of lithosphere: from the Pechora ocean to Timanian
1279 orogen, from the Paleouralian ocean to Uralian orogeny, in: Leonov, Y.G. (Ed.),
1280 Problems of Tectonics of the Central Asia. GEOS, Moscow, pp. 309–342 (In
1281 Russian).
1282 Puchkov, V.N., 2013. Structural stages and evolution of the Urals. Mineralogy and
1283 Petrology 106, 3–37.
1284 Puchkov, V.N., Bogdanova, S.V., Ernst, R.E., Kozlov, V.I., Krasnobaev, A.A., Soderlund,
1285 U., Wingate, M.T.D., Postnikov, A.V., Sergeeva, N.D., 2013. The ca. 1380 Ma
1286 Mashak igneous event of the Southern Urals. Lithos 174, 109-124.
1287 Puchkov, V.N., Krasnobaev, A.A., Kozlov, V.I., Sergeeva N.D., 2012. New isotope ages
1288 of volcanics in the standard section of the Riphean and Vendian of the Southern
1289 Urals: consequences for stratigraphy and tectonics, in: Materials for the 435 IX-th
1290 Republican Conference on Geology and Environment. Institute of Geology, Ufa,
1291 pp. 52–56.
1292 Pyatiletov, V.G., 1979. On finds of blue-green algae Yudoma deposits of Yakutia
1293 (Vendian). Doklady Academii Nauk SSSR 249, 714-716 (In Russian).
1294 Pyatiletov, V.G., 1988. Microfossils of the Late Proterozoic of the Uchur-Maya Region, in:
1295 Khomentovsky, V.V., Schenfil', V.Y. (Eds.), Late Precambrian and Early Paleozoic of
1296 Siberia. IGiG SO AN SSSR, Novosibirsk, pp. 47-104 (In Russian).
1297 Rippka, R., Deuellesj, J., Waterbury, J., Herdman, M., Stanier, R.Y., 1979. Generic
1298 assignments, strain histories, and properties of pure cultures of cyanobacteria.
1299 Journal of General Microbiology 111, 1-61.

1300 Schirrmeister, B.E., Gugger, M., Donoghue, P.C.J., 2015. Cyanobacteria and the Great
1301 Oxidation Event: evidence from genes and fossils. Palaeontology 58, 769-785.
1302 Schepeleva, E.D., 1960. Finds of blue-green algae in Lower Cambrian deposits of the
1303 Leningrad region, in: Problemy Neftyanoi Geologii i Voprosy Metodiki Laboratornykh
1304 Issledovanij. Nauka, Moscow, pp. 170-172 (In Russian).
1305 Schopf, J.W., 1968. Microflora of the Bitter Springs Formation, Late Precambrian, central
1306 Australia. Journal of Paleontology 42, 651–688.
1307 Schopf, J.W., 1992. Atlas of representative Proterozoic microfossils, in: Schopf, J.W.,
1308 Klein, C. (Eds.), The Proterozoic Biosphere. Cambridge University Press,
1309 Cambridge, 1055-1118.
1310 Sergeev, V.N., 1992. Silicified microfossils of the Precambrian and Cambrian of the Urals
1311 and Central Asia. Nauka, Moscow (in Russian).
1312 Sergeev, V.N., 2006. Precambrian microfossils in cherts: their paleobiology, classification,
1313 and biostratigraphic usefulness. Geos, Moscow (in Russian).
1314 Sergeev, V.N., 2009. The distribution of microfossil assemblages in Proterozoic rocks.
1315 Precambrian Research 173, 212–222.
1316 Sergeev, V.N., Lee Seong-Joo, 2001. Microfossils from cherts of the Middle Riphean
1317 Svetlyi Formation, the Uchur-Maya Region of Siberia and their stratigraphic
1318 significance. Stratigraphy and Geological Correlation 9, 1-10.
1319 Sergeev, V.N., Lee Seong-Joo, 2004. New data on silicified microfossils from the Satka
1320 Formation of the Lower Riphean Stratotype, the Urals. Stratigraphy and Geological
1321 Correlation 12, 1-21.
1322 Sergeev, V.N., Krylov, I.N., 1986. Microfossils of the Min'yar Formation from the Basin
1323 of Inzer River. Paleontological Journal 1, 84-95 (In Russian).

1324 Sergeev, V.N., Schopf, J.W., 2010. Taxonomy, paleoecology and biostratigraphy of the
1325 Late Neoproterozoic Chichkan Microbiota of South Kazakhstan: The Marine
1326 biosphere on the eve of metazoan radiation. Journal of Paleontology 84, 363-401.
1327 Sergeev, V.N., Knoll, A.H., Grotzinger, J.P., 1995. Paleobiology of the Mesoproterozoic
1328 Billyakh Group, Anabar Uplift, northeastern Siberia. Palaeontological Society
1329 Memoir 39, 1-37.
1330 Sergeev, V.N., Vorob'eva, N.G., Petrov, P.Yu., 2007. New Riphean microbiotas of the
1331 Billyakh Group, the North Anabar region (Fomich River Basin): Riphean
1332 biostratigraphy of the Siberian Platform. Stratigraphy and Geological Correlation
1333 15, 1-11.
1334 Sergeev, V.N., Semikhatov, M.A., Fedonkin, M.A., Vorob'eva, N.G., 2010. Principal
1335 stages in evolution of Precambrian organic world: Communication 2. The Late
1336 Proterozoic. Stratigraphy and Geological Correlation 18, 561-592.
1337 Sergeev, V.N., Knoll, A.H., Vorob'eva, N.G., 2011. The organic-wall compression-
1338 preserved microfossils from the Ediacaran Ura Formation of the Baikal-Patom
1339 Uplift, Siberia: taxonomy and biostratigraphic significance. Journal of
1340 Paleontology 85, 987-1011.
1341 Sergeev, V.N., Sharma, M., Shukla, Y., 2008. Mesoproterozoic silicified microbiotas of
1342 Russia and India – characteristics and contrasts. Palaeobotanist 57, 323-358.
1343 Sergeev, V.N., Sharma, M., Shukla, Y., 2012. Proterozoic fossil cyanobacteria.
1344 Palaeobotanist 61, 189-358.
1345 Shatsky, N.S., 1964. Selected works 2. Nauka, Moscow (In Russian).
1346 Singh, V.K., Sharma, M., 2014. Morphologically complex organic-walled microfossils
1347 (OWM) from the late Paleoproterozoic – early Mesoproterozoic Chitrakut
1348 Formation, Vindhyan Supergroup, Central India and their implications on the
1349 antiquity of eukaryotes. Journal of the Paleontological Society of India 59, 89-102.

1350 Sperling, E.A., Rooney, A.D., Hays, L., Sergeev, V.N., Vorob'eva, N.G., Sergeeva, N.D.,
1351 Selby, D., Johnston, D.T., Knoll, A.H., 2014. Redox heterogeneity of subsurface
1352 waters in the Mesoproterozoic ocean. Geobiology 12, 373–386.
1353 Sperling, E.A., Wolock, C.J., Morgan, A.S., Gill, B.C., Kunzmann, M., Halverson, G.P.,
1354 Macdonald, F.A., Knoll, A.H., Johnston, D.T., 2015. Statistical analysis of iron
1355 geochemical data suggests limited late Proterozoic oxygenation. Nature 523, 451-
1356 454.
1357 Stueeken, E.E., 2013. A test of the nitrogen-limitation hypothesis for retarded eukaryote
1358 radiation: nitrogen isotopes across a Mesoproterozoic basinal profile. Geochimica
1359 et Cosmochimica Acta 120, 121-139.
1360 Sun, W.G., 1987. Palaeontology and biostratigraphy of Late Precambrian macroscopic
1361 colonial algae: *Chuaria* Walcott and *Tawuia* Hofmann. Palaeontographica B 203,
1362 109-134.
1363 Talyzina, N., Moczydłowska, M., 2000. Morphological and ultrastructural studies of some
1364 acritarchs from the Lower Cambrian Lukati Formation, Estonia. Review of
1365 Palaeobotany and Palynology 112, 1-21.
1366 Tang, Q., Pang, K., Xiao, S., Yuan, X., Oua, Z., Wan, B., 2013. Organic-walled
1367 microfossils from the early Neoproterozoic Liulaobei Formation in the Huainan
1368 region of North China and their biostratigraphic significance. Precambrian
1369 Research 236, 157– 181.
1370 Tappan, H., 1980. The Paleobiology of Plant Protists. WH Freeman, San Francisco.
1371 Teyssèdre, B., 2006. Are the green algae (phylum Viridiplantae) two billion years old?
1372 Carnets de Geologie 3, 1–21.
1373 Timofeev, B.V., 1966. Micropaleontological investigation of ancient formations. Nauka,
1374 Moscow (In Russian).
1375 Timofeev, B.V., 1969. Proterozoic Spheromorphida. Nauka, Leningrad (In Russian).

1376 Timofeev, B.V., Herman, T.N., 1979. Precambrian microbiota of the Lakhanda Formation,
1377 in: Sokolov, B.S. (Ed.), Paleontology of the Precambrian and Early Cambrian.
1378 Nauka, Leningrad, pp. 137-147 (in Russian).
1379 Timofeev, B.V., Herman, T.N., Mikhailova, N.S., 1976. Microphytofossils from the
1380 Precambrian, Cambrian and Ordovician. Nauka, Leningrad (In Russian).
1381 Thusu, B., 1973. Acritarches provenant de l'Ilion Shale (Wenlockian), Utica, New York.
1382 Revue de Micropaléontologie 16, 137-146.
1383 Tynni, R., Donner, J., 1980. A microfossil and sedimentation study of the late Precambrian
1384 formation of Hailuoto, Finland. Geological Survey of Finland 311, 1-27.
1385 Veis, A.F., 1984. Microfossils from the Upper Riphean of the Turikhansk region.
1386 Paleontological Journal 2, 102-108 (In Russian).
1387 Veis, A.F., Vorob'eva, N. G., 1992. Riphean and Vendian microfossils from the Anabar
1388 Uplift. Izvestiya AN SSSR, Seriya Geologicheskaya 1, 114-130 (In Russian).
1389 Veis, A.F., Petrov, P.Yu., 1994a. The main peculiarities of the environmental distribution
1390 of microfossils in the Riphean Basins of Siberia. Stratigraphy and Geological
1391 Correlation 2, 397-425.
1392 Veis, A.F., Petrov, P.Yu., 1994b. Taxonomic diversity of Riphean organic-walled
1393 microfossils as dependent on their origination settings (the Bezymyannyi Formation
1394 of Turukhansk Region as an example), in: Ecosystem Reorganizations and
1395 Evolution of Biosphere 1. Nedra, Moscow, pp. 32–42.
1396 Veis, A.F., Semikhatov, M.A., 1989. The Lower Riphean Omakhta microfossil assemblage of
1397 Eastern Siberia: composition and depositional environments. Izvestiya AN SSSR,
1398 Seriya Geologicheskaya 5, 36–55 (In Russian).
1399 Veis, A.F., Kozlova, E.V., Vorob'eva, N.G., 1990. Organic-walled microfossils from the type
1400 section of the Riphean (Southern Urals). Izvestiya AN USSR, Seria Geologicheskaya 9,
1401 20-36 (In Russian).

1402 Veis, A.F., Petrov, P.Yu., Vorob'eva, N.G., 2001. Geochronological and biostratigraphic
1403 approaches to reconstruction of Precambrian biota evolution: new finds of microfossils
1404 in Riphean sections on the Western Slope of the Anabar Uplift. Doklady Earth
1405 Sciences 378(4), 413-419.

1406 Veis, A.F., Larionov, N.N., Vorob'eva, N.G., Lee Seong-Joo, 2000. Significance of
1407 microfossils for Riphean stratigraphy of the Southern Urals (Bashkirian
1408 Meganticlinorium) and adjacent region (Kama-Belaya Aulacogen). Stratigraphy
1409 and Geological Correlation 8, 33–50.

1410 Vidal., G., 1976. Late Precambrian microfossils from the Visingsö Beds in southern
1411 Sweden. Fossils and Strata 9, 1-56.

1412 Vidal, G., Ford, T.D., 1985. Microbiotas from the Late Proterozoic Chuar Group (Northern
1413 Arizona) and Uinta Group (Utah) and their chronostratigraphic implications.
1414 Precambrian Research 28, 349–389.

1415 Villalobo, E., Moch, C., Fryd-Versavel, G., Fleury-Aubusson, A., Morin, L., 2003.
1416 Cysteine proteases and cell differentiation: excystment of the ciliated protist
1417 *Sterkiella histriomuscorum.* Eukaryotic Cell 2, 1234–1245

1418 Vorob'eva, N.G., Sergeev, V.N., Semikhatov, M.A., 2006. Unique Lower Vendian
1419 Kel'tma microbiota, Timan Ridge: new evidence for the paleontological essence
1420 and global significance of the Vendian System. Doklady Earth Sciences 410, 1038-
1421 1043.

1422 Vorob'eva, N.G., Sergeev, V.N., Knoll, A.H., 2009. Neoproterozoic microfossils from the
1423 northeastern margin of the East European Platform. Journal of Paleontology 83,
1424 161-192.

1425 Vorob'eva, N.G., Sergeev, V.N., Petrov, P.Yu., 2015. Kotuikan Formation assemblage: A
1426 diverse organic-walled microbiota in the Mesoproterozoic Anabar succession,
1427 northern Siberia. Precambrian Research 256, 201-222.

1428 Walcott, C.D., 1899. Precambrian fossiliferous formations. Geological Society of America
1429 Bulletin 10, 199-244.
1430 Wellman, C.H., Strother, P.K., 2015. The terrestrial biota prior to the origin of land plants
1431 (embryophytes): a review of the evidence. Palaeontology 58, 601-627.
1432 Willman, S., Moczydlowska, M., 2008. Ediacaran acritarch biota from the Giles 1 drillhole,
1433 Officer Basin, Australia, and its potential for biostratigraphic correlation.
1434 Precambrian Research 162, 498-530.
1435 Wiman, C., 1894. Ein prakambrisches Fossil. Bulletin of the Geological Institution of the
1436 University of Uppsala 2, 109-113.
1437 Xiao, S., Knoll, A.H., Kaufman, A.J., Yin, L., Zhang, Y., 1997. Neoproterozoic fossils in
1438 Mesoproterozoic rocks? Chemostratigraphic resolution of a biostratigraphic
1439 conundrum from the North China Platform. Precambrian Research 84, 197-220.
1440 Yankauskas, T.V., 1980. On the micropaleontlogical characteristic of the Middle and
1441 Upper Cambrian in the north-west of the East European Platform. Izvestiya
1442 Akademiya Nauk Estonskoyi SSR, Geology 19(4), 131-135 (In Russian).
1443 Yankauskas, T.V., 1982. Microfossils of the Riphean in the Southern Urals, in: Keller, B.M.
1444 (Ed.), Stratotype of the Riphean. Palaeontology, Palaeomagnetism. Nauka, Moscow, pp.
1445 84–120 (In Russian).
1446 Yankauskas, T.V. (Ed.), 1989. Precambrian microfossils of the USSR. Trudy Instituta
1447 Geologii i Geochronologii Dokembria SSSR Akademii Nauk, Leningrad (In
1448 Russian).
1449 Yin, L., 1997. Acanthomorphic acritarchs from Meso-Neoproterozoic Shales of the Ruyang
1450 Group, Shanxi, China. Review of Palaeobotany and Palynology 98, 15–25.
1451 Yin, L., Yuan, X., Meng, F., Hu, J., 2005. Protista of Upper Mesoproterozoic Ruyang
1452 Group in Shanxi Province, China. Precambrian Research 141, 49-60.

1453 Zhang, R., Feng, S., Ma, G., Xu, G., Yan, D., 1991. Late Precambrian macroscopic fossil
1454 algae from Hainan Island. Acta Palaeontologica Sinica 30, l l5-l25.
1455 Zhang, Y., 1981. Proterozoic stromatolite microfloras of the Gaoyuzhuang Formation
1456 (Early Sinian: Riphean), Hebei, China. Journal of Paleontology 55, 485–506.
1457

Figure captions

Fig. 1. A – Index map of North Eurasia, indicating the location of the studied area (filled square at arrow). B – Map of the southern Ural Mountains and Volgo-Ural region showing the locations of the microfossiliferous boreholes of the Kaltasy Formation (filled pentagons; see section 3.1 for details), abbreviations: 203B – 203 Bedryazh, 133AP – 133 Azino-Pal'nikovo, and 1EA – 1 East Askino boreholes.

Fig. 2. Generalized Proterozoic stratigraphy of the Bashkirian meganticlinorium (southern Ural Mountains) and Volga–Ural region (upper Neoproterozoic part of the successions not shown) with 1 East Askino (1EA), 203 Bedryazh (203B) and 133 Azino-Pal'nikovo (133AP) boreholes (modified after Keller and Chumakov, 1983; Sergeev, 2006; Kah et al., 2007; Kozlov et al., 2011). Abbreviations, formations and members: Ai-Bin – Ai-Bolshoi Inzer, St-Sr – Satka-Suran, Bk-Js – Bakal-Yusha, Ms – Mashak, Zg – Zigal'ga, Zk – Zigazy-Komarovo, Av – Avzyan, Zl – Zilmerdak, Kt – Katav, In – Inzer, Sg - Sigaevo, Ks - Kostino, Nr – Norkino, Rt – Rotkovo, Mn – Minaevo, Kl – Kaltasy, Kl_1 – Sauzovo, Kl_2 – Arlan, Kl_3 – Ashit, Kb – Kabakovo, Nd – Nadezhdino, Tk – Tukaevo, Ol – Ol'khovka, Us – Usa, Ln – Leonidovo, Pr – Priyutovo; Sh – Shikhan, Lz – Leuznovo; groups and subgroups: Sr – Sarapul, Pk – Prikamskii, Br –Borodulino; other geological units: PP – Paleoproterozoic, LP – Lower Proterozoic, Pz – Paleozoic, R_2 – Middle Riphean, Ed – Ediacaran, V – Vendian. Key, 1 – tillites, 2 – conglomerates, 3 – sandstones, 4 – siltstones, 5 – shales, 6 – limestone, 7 – clay limestone, 8 – dolomite, 9 – dolomites with cherts, 10 – marls, 11 – stromatolites, 12 – *Conophyton* stromatolites, 13 – tuff, tuffaceous sandstone, and diabase; 14 – basement gneiss, 15 – disconformities, 16 – angular unconformities. New Re–Os age estimates from 203 Bedryazh core (Sperling et al., 2014) indicated by arrow (see section 2.3 for details). The numbers of the collected samples are shown to the right of the

1EA and 203B cores (indicated by dots); fossiliferous levels of the samples collected by Veis et al., 2000 are indicated to the left of 133AP core (arrows). The fossiliferous Arlan (Kl_2) and Ashit (Kl_3) members of the Kaltasy Formation are shown with different shades of grey.

Fig. 3. Microfossil taxa reported from the Kaltasy Formation, indicating their morphological grouping, relative abundance (R = rare, C = common, D = dominant), and size range (displayed on a logarithmic scale in which the arrows denote taxa larger than 550 µm in diameter).

Fig. 4. Sphaeromorph acritarchs. 1, 6, 7, *Leiosphaeridia jacutica*; 1, (1EA)-11-3, p. 6, P55[3], 14712-117; 6, (1EA)-15-1, p. 2, M52[3], 14712-191; 7, (1EA)-11-4, p. 5, R50[0], 14712-124; 2, *Leiosphaeridia tenuissima* (large light disc) and *L. crassa* (smaller darker disk), (1EA)-12-3, p. 2, N59[2], 14712-154a and 14712-154b, respectively; 3, 4, *Leiosphaeridia ternata*; 3, (1EA)-16-1, p. 2, M54[0], 14712-196; 4, (203B)-40-1, p. 4, N70[2], 14712-70; 5, *Leiosphaeridia atava*, (203B)-40-3, p. 7, K66[0], 14712-92; 8 – 10, *Leiosphaeridia* sp.; 8, (1EA)-16-6, p. 2, M49[4], 14712-228; 9, (1EA)-12-2, p. 2, M46[2], 14712-147; 10, (1EA)-11-3, p. 3, M62[1], 14712-114; 11 – 13, *Leiosphaeridia* (?) *wimanii*; 11, (203B)-34-20, p. 1, R27[3], 14712-297; 12, (203B)-34-19, p. 2, M61[2], 14712-296; 13, (203B)-34-19, p. 1, L62[4], 14712-298. For all illustrated specimens, the single scale bar = 10 µm and the double bar = 100 µm. All specimens are from the Arlan and Ashit members of the Kaltasy Formation; sample location and explanation are provided in sections 3.1 and 7.1, respectively.

1508 Fig. 5. Sphaeromorph and netromorph acritarchs.1, *Spumosina rubiginosa*, (133AP)-2560-
1509 2568, p. 1, K38[2], 14712-287; 2, 3, *Synsphaeridium* sp.; 2, (203B)-31-1, p. 2, Q59[3],
1510 14712-8; 3, (1EA)-18-1, p. 4, N59[4], 14712-243; 4-7, *Pterospermopsimorpha pileiformis*;
1511 4, (1EA)-11-1, p. 3, N53[4], 14712-104; 5, (1EA)-11-4, p. 1, K51[2], 14712-120; 6, (1EA)-
1512 14-1, p. 1, L48[0], 14712-186; 7, (1EA)-12-4, p. 4, Q58[4], 14712-165; 8, 9, *Spiromorpha*
1513 aff. *S. segmentata,* (203B)-34-6, p. 1, M64[3],14712-32; 9, detail of 8, arrows indicate
1514 crescent-like connecting wields; 10-12, (?)*Moyeria* sp.; 10, 11, (203B)-34-6, p. 3, S59[2],
1515 14712-34, 11, detail of 10, arrows indicate overlapping of bispiral bands each to other;12,
1516 (1EA)-12-4, p. 3, O57[2], 14712-164, arrows indicate possible initial cleavage of vesicle;
1517 13-15, *Navifusa* sp.; 13, (1EA)-16-8, p. 3, M58[4], 14712-235; 14, (1EA)-11-2, p. 4,
1518 N58[4], 14712-110; 15, (1EA)-12-1, p. 3, O53[1], 14712-136.

1519

1520 Fig. 6. Large filamentous forms. 1-6, *Rectia magna*; 1, (133AP)-2064-2068-1, p. 2,
1521 H40[3], 14712-6802; 2, (133AP)-2052-2054-1, p. 3, J36[1], 14712-5084; 3, holotype,
1522 (133AP)-2052-2054-1, p. 8, Q33[2], 14712-5408; 4, (133AP)-2056-2058-1, p. 4, Q47[2],
1523 14712-269; 5, (133AP)-2058-2060-1, p. 2, K38[2], 14712-6002; 6, (133AP)-2052-2054-1,
1524 p. 9, Y40[4], 14712-265; 7–9, *Eosolena minuta*; 7, (1EA)-11-5, p. 1, L46[0], 14712-125, 8,
1525 9, details of 9; 10, *Plicatidium latum,* (133AP)-2044-2046-1, p. 6, O41[1], 14712-4618;
1526 11, 12, *Rugosoopsis* sp.; 11, (133AP)-2073-2077-1, p. 3, K44[4], 14712-279; 12, (203B)-
1527 34-7, p. 1, L67[2], 14712-35.

1528

1529 Fig. 7. Filamentous microfossils. 1, *Polytrichoides* aff. *P. lineatus,* (133AP)-2060-2064-1,
1530 p. 1, D36[3], 14712-6401; 2, 6, 7, *Oscillatoriopsis longa*; 2, (133AP)-2044-2046-1, p. 2,
1531 D45[3], 14712-258; 6, (1EA)-11-5, p. 3, J45[4], 14712-131; 7, (203B)-39-3, p. 2, L68[1],
1532 14712-60; 3, 5, *Tortunema patomica;* 3, (1EA)-11-3, p. 4, N59[3], 14712-115; 5, (133AP)-

2058-2060-1, p. 12, K39[2], 14712-271; 4, 8, *Cephalonyx* sp.; 4, (133AP)-2568-2572-1, p. 6, N40[2], 14712-6003; 8, (133AP)-2073-2077-1, p. 1, G36[3], 14712-278, arrow indicates a probable mechanically displaced trichome fragment.

Fig. 8. Filamentous and miscellaneous microfossils. 1-3, *Pseudodendron anteridium;* 1,(133AP)-2817-2822-1, p. 2, V20[1], 14712-2801; 2, (133AP)-2760-2765-1, p. 4, H36[3], 14712-2764; 3, (203B)-40-3, p. 1, E57[3], 14712-86; 4, *Siphonophycus robustum* (thin threads) and poorly preserved filaments of *Polytrichoides* aff. *P. lineatus* or *Pellicularia tenera* (larger threads), (203B)-34-3, p. 4, Q59[1], 14712-24; 5, *Siphonophycus typicum,* (1EA)-12-7, p. 1, M53[3], 14712-184; 6, *Siphonophycus solidum,* (1EA)-11-3, p. 2, L57[3], 14712-113; 7, *Siphonophycus punctatum,* (133AP)-2046-2048-1, p. 1, F35[4], 14712-4803; 8-10, *Pellicularia tenera;* 8, (133AP)-2353-2355-1, p. 1, W44[2], 14712-551; 9, (203B)-34-9, p. 2, K66[4], 14712-43; 10, (203B)-34-8, p. 3, P68[4], 14712-41.

Fig. 9. Miscellaneous microfossils. 1–3, Unnamed form 1; 1, (1EA)-12-6, p. 2, N46[3], 14712-182; 2, (1EA)-12-2, p. 5, K57[3], 14712-150; 3, (1EA)-12-3, p. 1, F60[4], 14712-153; 4 – 6, Unnamed form 2; 4, (203B)-31-1, p. 3, S60[1], 14712-9; 5, (203B)-39-3, p. 3, M69[4], 14712-61; 6, (203B)-34-3, p. 3, K60[4], 14712-23; 7, 10, Unnamed form 3; 7, (203B)-40-2, p. 7, R53[4], 14712-83; 10, (203B)-40-2, p. 8, S58[3], 14712-85; 8, 9, 11, 12, Unnamed form 4; 8, (1EA)-16-7, p. 2, N22[3], 14712-232; 9, (1EA)-16-2, p. 3, P55[4], 14712-205; 11, (203B)-34-3, p. 2, K62[0], 14712-22; 12, (1EA)-11-5, p. 1a, K47[3], 14712-126; 13, 14, Unnamed form 5; 13, (1EA)-12-3, p. 5, N53[4], 14712-158; 14, (1EA)-18-1, p. 6, O54[0], 14712-245.

Fig. 10. Three morphological groups (genera) of filamentous microfossils: A – *Rectia* tubes with a rounded closed end bearing double annulations, B – *Cephalonyx* tubes bearing numerous annulations, C – elastic tubes of *Tortunema* with numerous cross-ribs tapering toward both ends and poorly preserved trichome remains. The double scale bar is 100 µm and single bar is 10 µm.

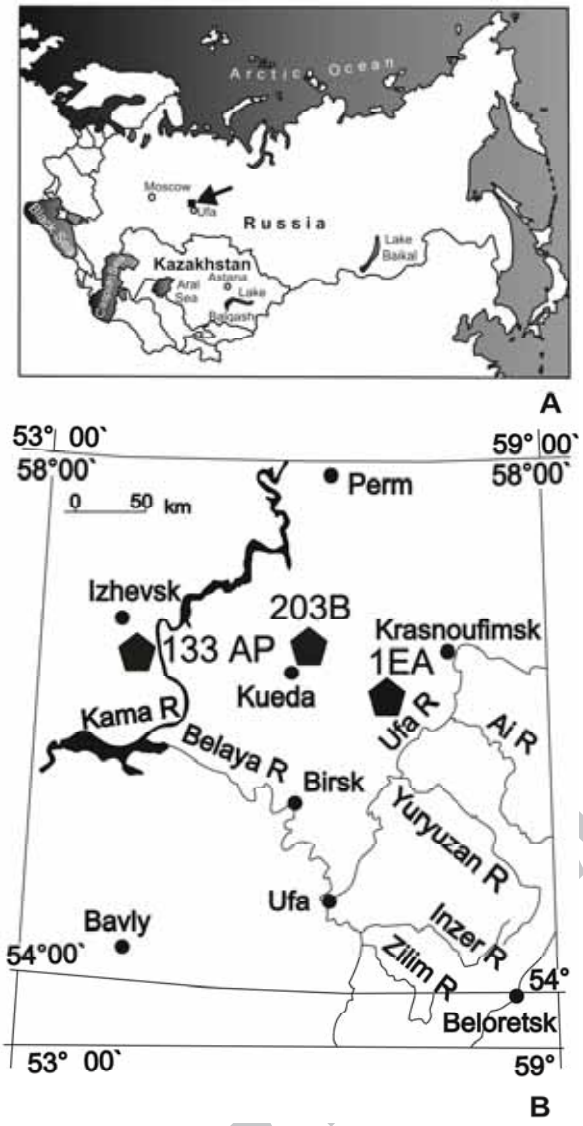

1565

1566

1567

1568 Fig. 1

1569

1570

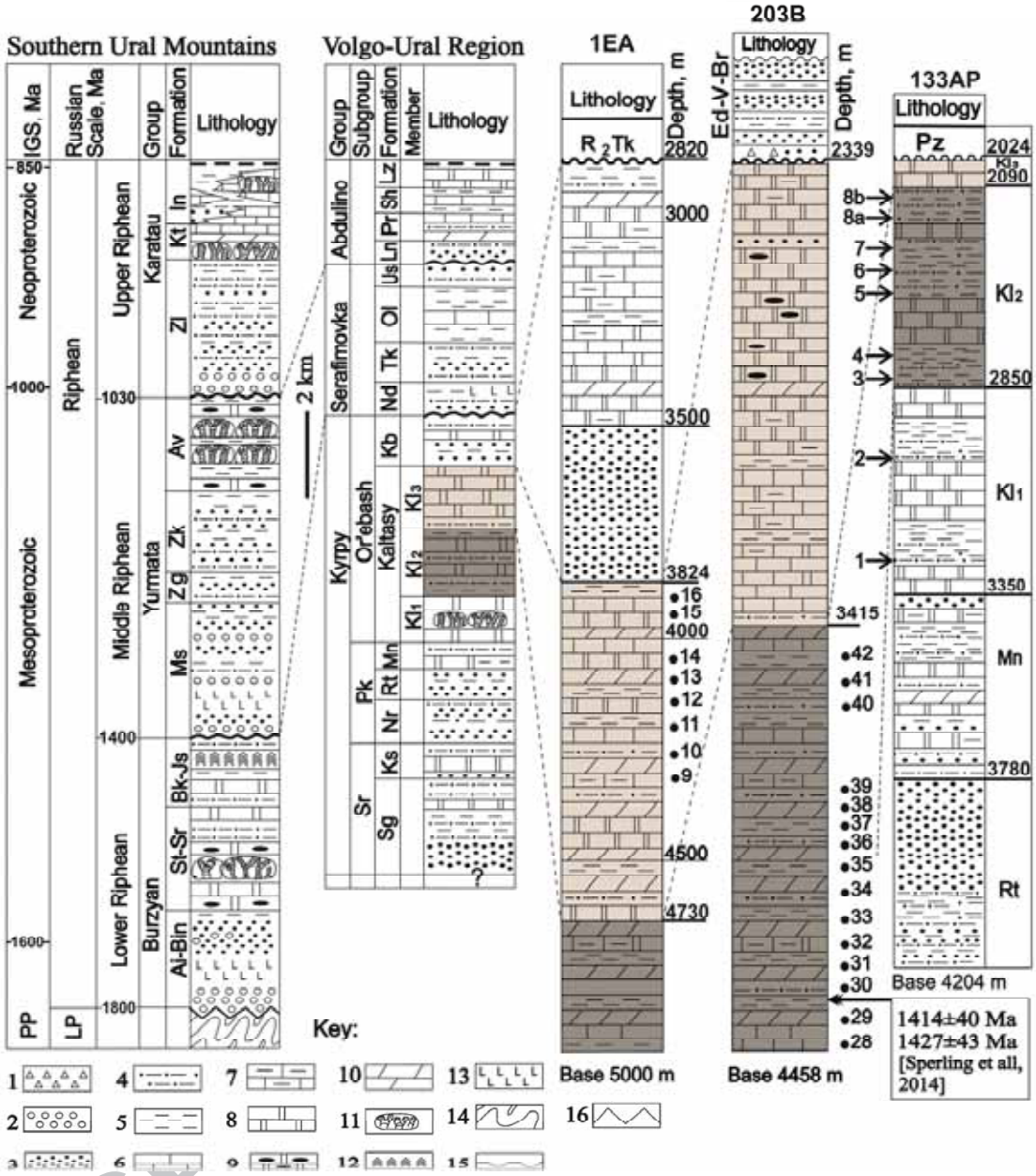

1571

1572

1573 Fig. 2

1574

1575

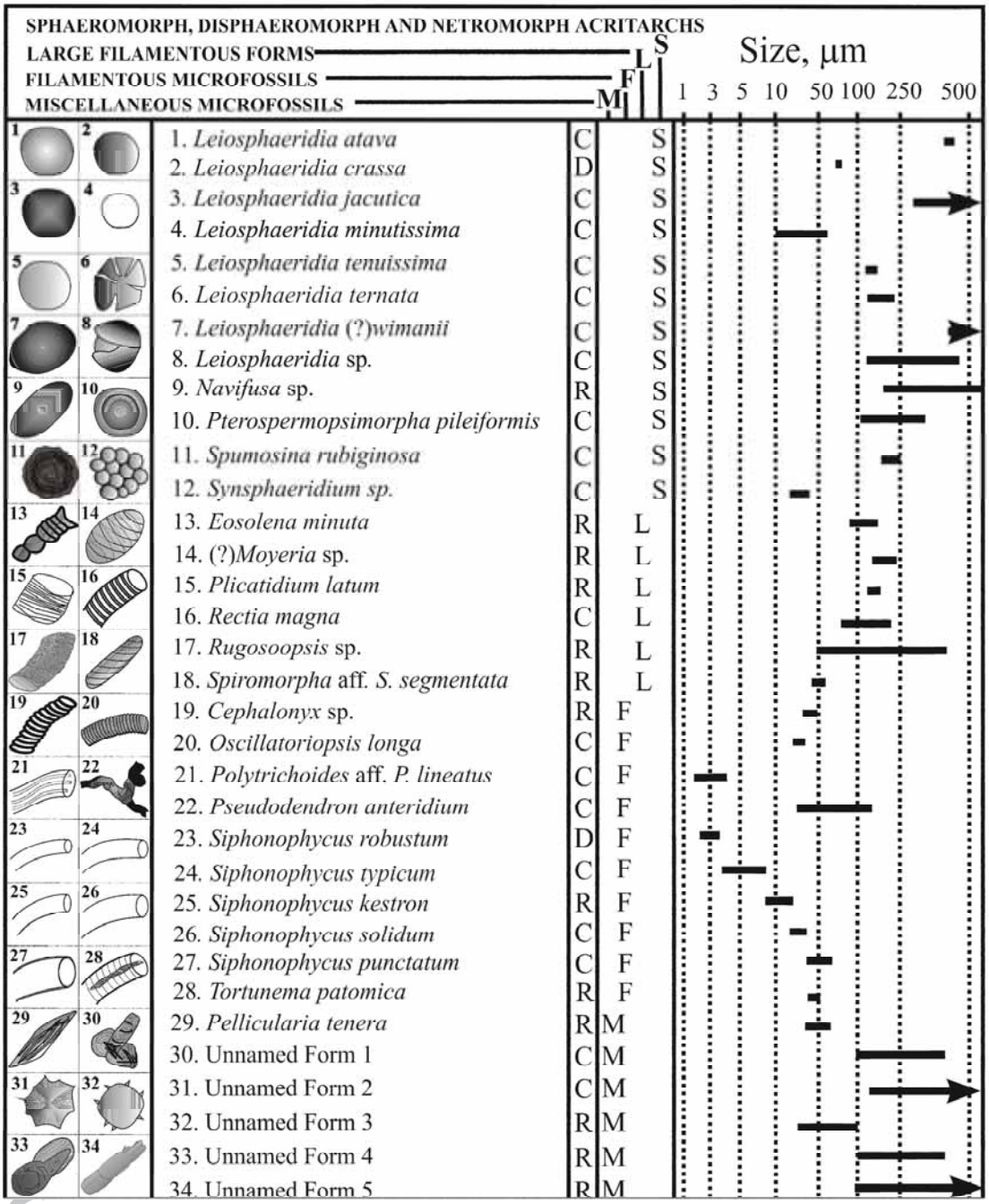

Fig. 3

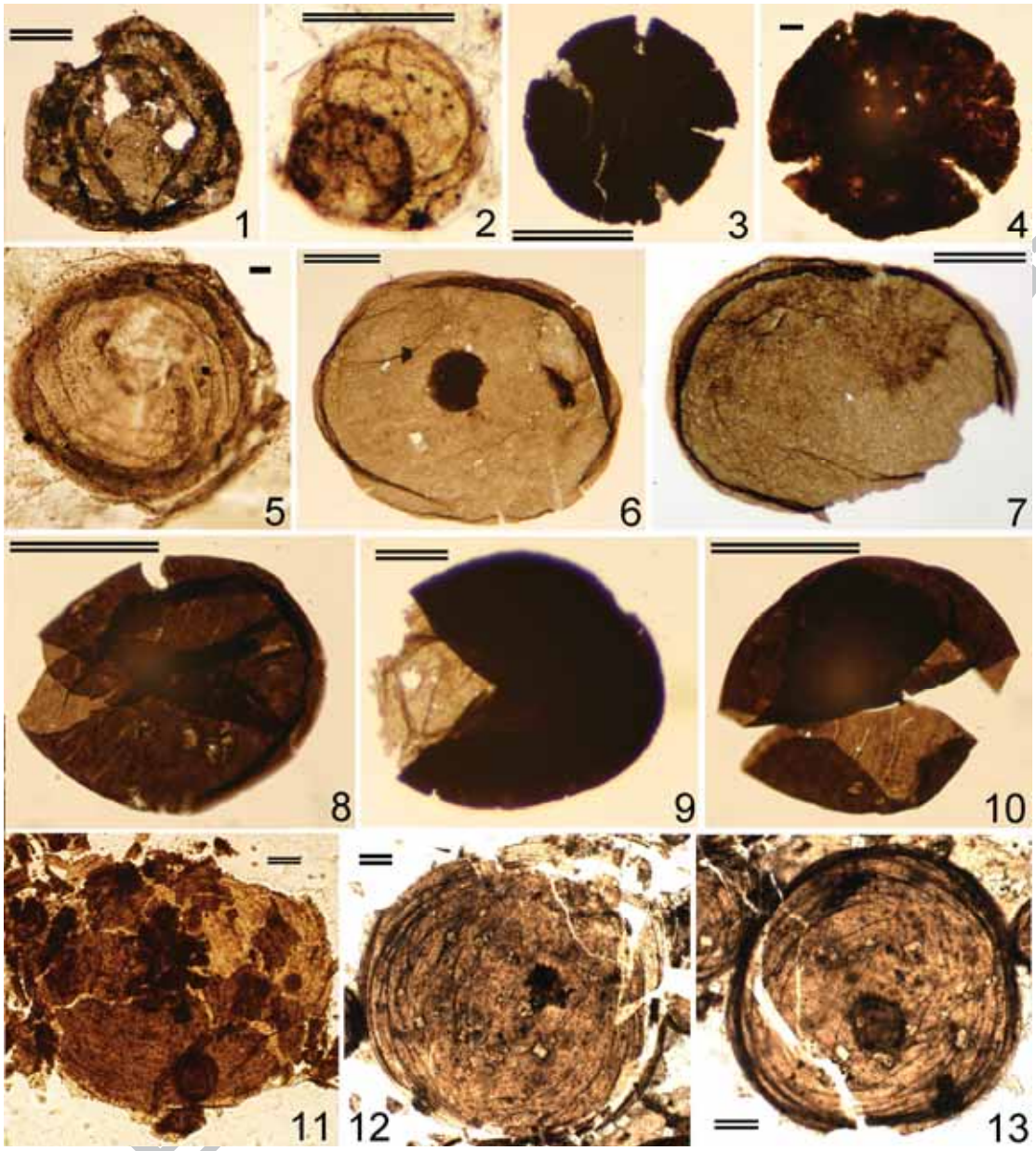

1582

1583

1584 Fig. 4

1585

1586

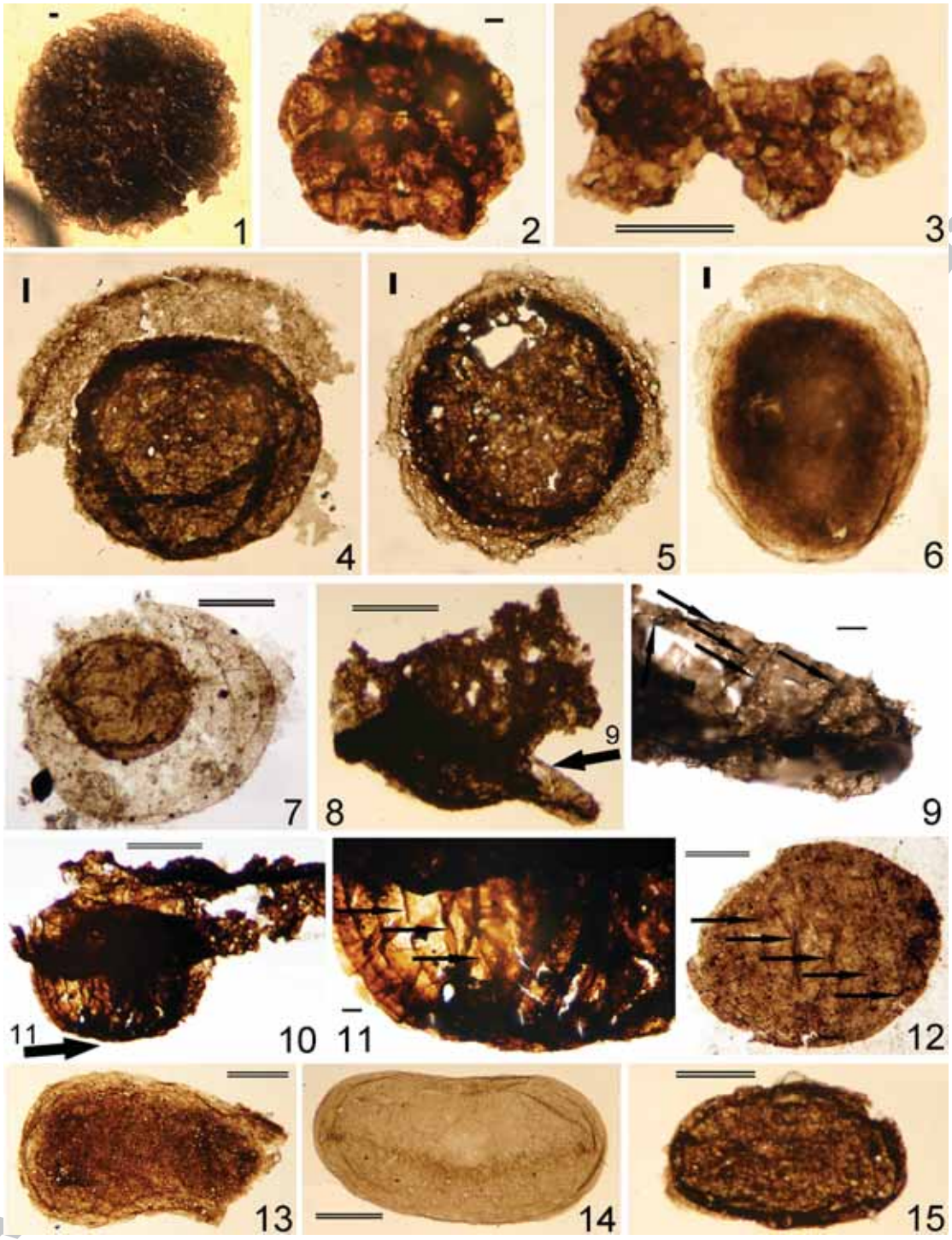

1587

1588

1589

1590 Fig. 5

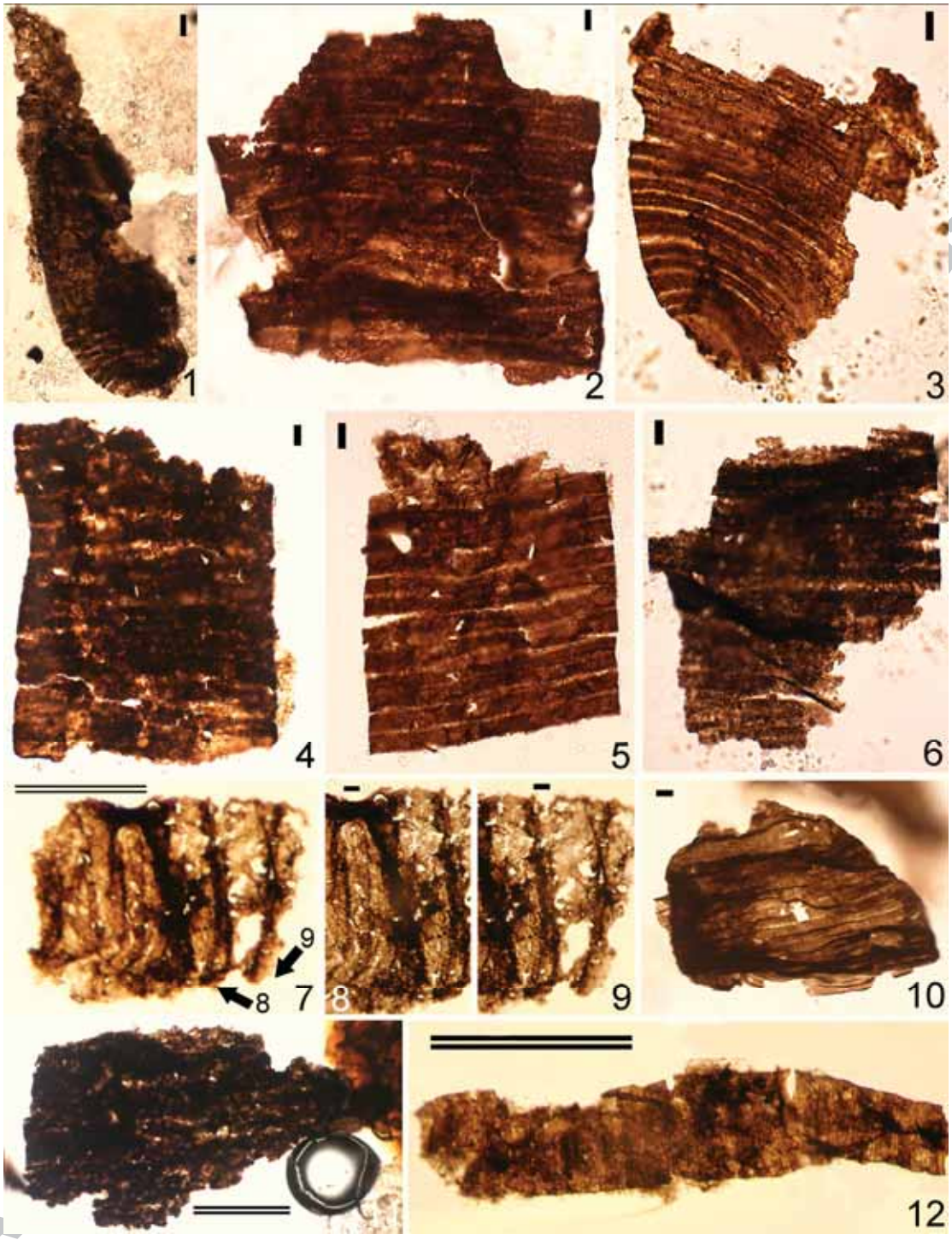

1591

1592

1593

1594 Fig. 6

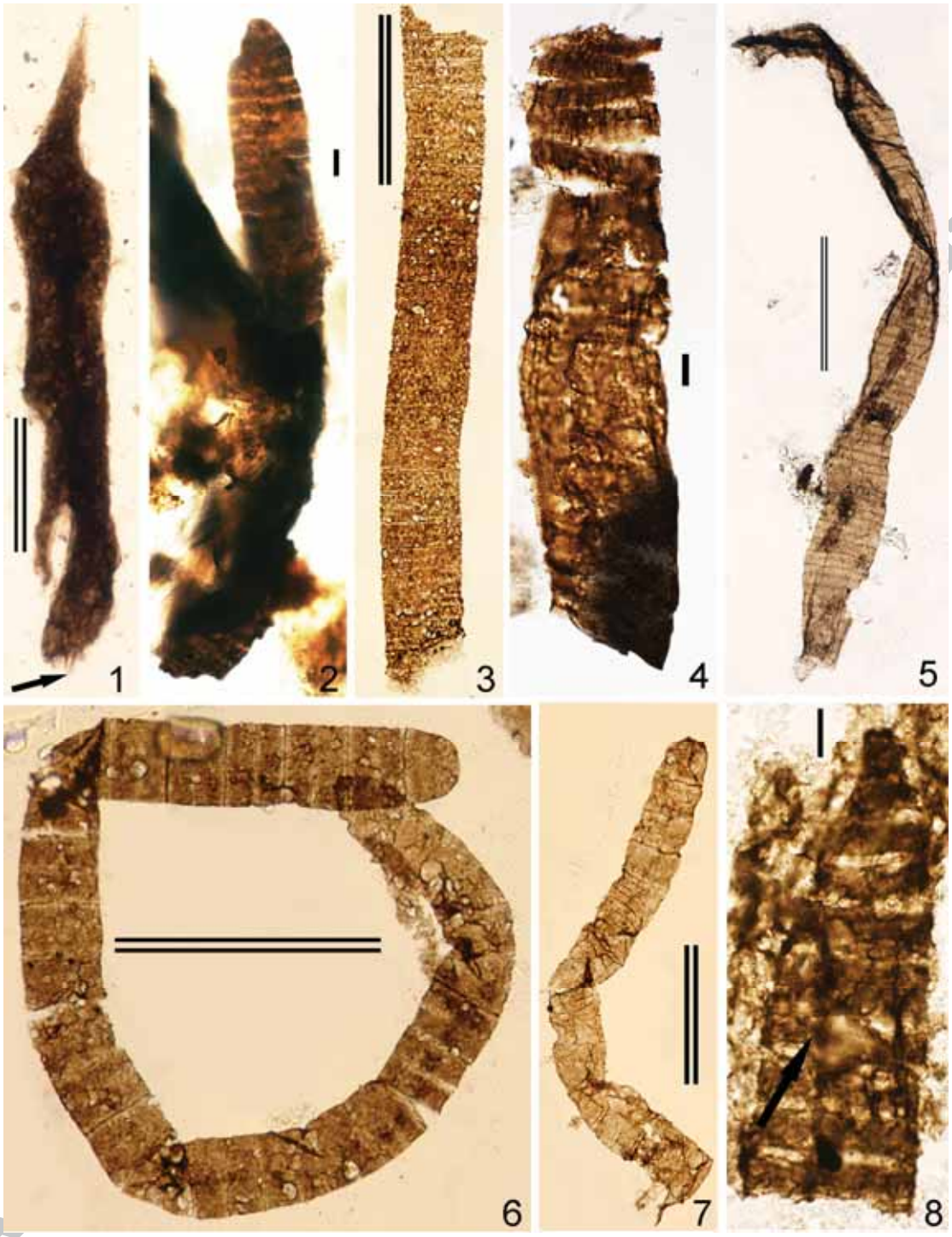

Fig. 7

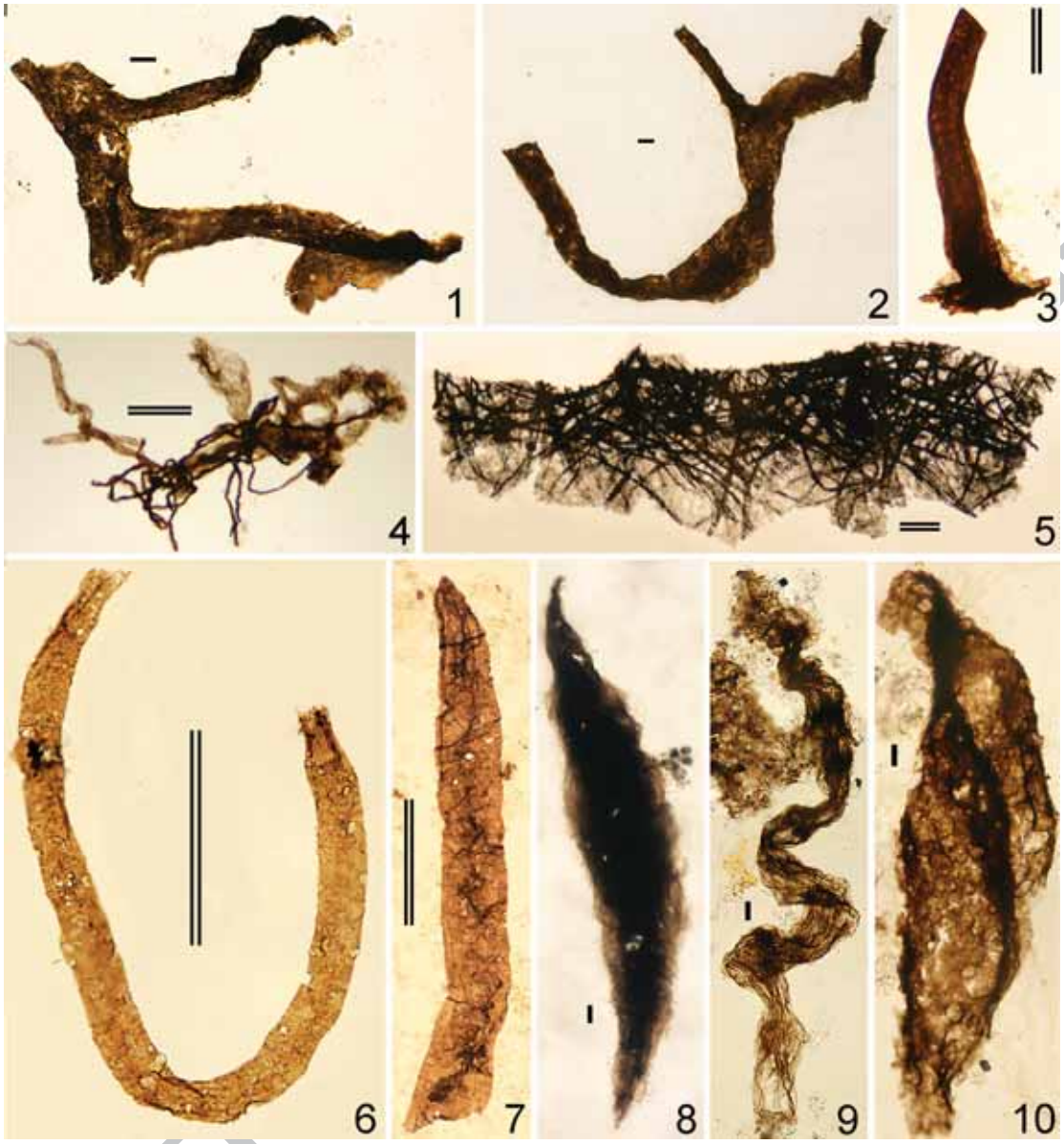

1599

1600

1601

1602 Fig. 8

1603

1604

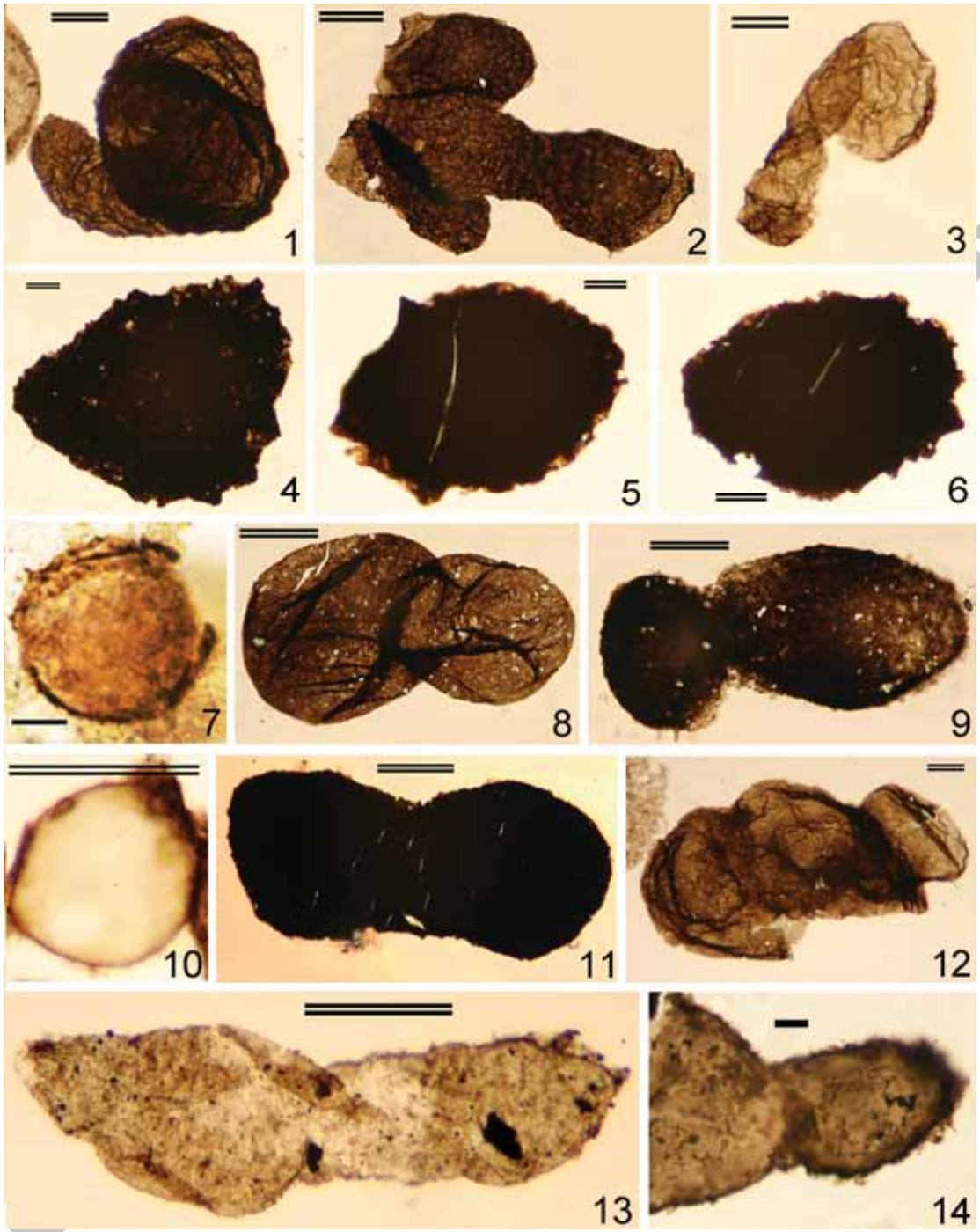

1605

1606

1607 Fig. 9

1608

1609

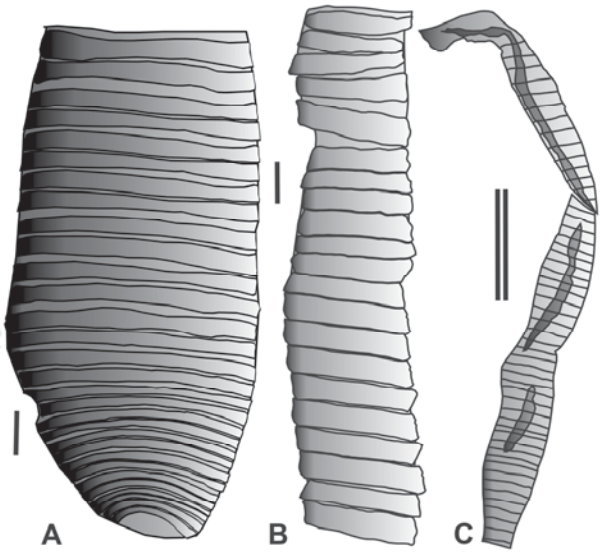

1610

1611

1612

1613 Fig. 10

1614

1615

1616

1617

1618 Graphical abstract

1619

1620

1621

1622

1623

1624 • The ~1450-Ma-old Kaltasy Formation contains compressed organic-walled microfossils.

1625

1626 • The fossils record life in basinal but oxic environments.

1627

1628 • The assemblage includes large and moderately complex eukaryotic microorganisms.

1629

1630 • The microbiota differs from many coeval deposits in its absence of acanthomorphs.

1631

1632 • The fossils document morphological conservatism among early eukaryotes.

1633

1634